

Bielefeld University

Faculty of Physics

Masters thesis

The duration of cosmological inflation

Pascal Kreling

pkreling@physik.uni-bielefeld.de

Bielefeld University

Wertherstraße 442, 33619 Bielefeld

Germany

Supervisor and 1st Referee:

Prof. Dr. Dominik J. Schwarz

dschwarz@physik.uni-bielefeld.de

Bielefeld University

2nd Referee:

Dr. Yuko Urakawa

yuko@physik.uni-bielefeld.de

Bielefeld University

October 14, 2019

Contents

Notation	1
1 Introduction	2
2 From Big Bang to galaxy structures	6
2.1 Λ CDM - Standard model of cosmology	6
2.2 Observations - Studying the Universe experimentally	14
2.3 Cosmological inflation - Seeds for structure formation	19
2.3.1 The inflaton field	20
2.3.2 The number of e-folds	21
2.3.3 Curing weaknesses of the Λ CDM-model	22
2.3.4 Thermal history of the Universe	23
3 Revisiting the number of e-folds of inflation	30
3.1 Deriving the exact value	31
3.1.1 Sudden reheating	31
3.1.2 Including a reheating process	33
3.2 Change in the reconstruction of number of e-folds due to other effects	34
3.2.1 Influence of measurement errors	34
3.2.2 Deviation from slow-roll inflation	37
3.2.3 Change in the equation of state of Dark Energy	38
4 Slow-roll evolution	40
5 Conclusion and outlook	45
References	46

Notation

In this work, the (pseudo-)metric tensor for flat space-time with the convention known as mostly-plus is used, i.e. $\eta^{00} = -1$ and $\eta^{11} = \eta^{22} = \eta^{33} = 1$. Therefore, the scalar product of two four vectors x^μ is

$$x^\mu x_\mu = x^\mu x^\nu \eta_{\mu\nu} = -\left(x^0\right)^2 + (\vec{x})^2. \quad (0.1)$$

Here, the Einstein sum convention is used.

All calculations use natural units $c = \hbar = k_B = 1$, where c is the vacuum speed of light, \hbar is the reduced Planck constant and k_B is the Boltzmann constant.

A dot over any quantity, e.g. \dot{a} , denotes a derivative with respect to cosmic time.

Introduction

1

Current methods of analysing measurements of the Cosmic Microwave Background (CMB) to constrain cosmic inflation are not precise enough for future observations and still have the weakness to introduce an arbitrary potential of the inflationary model. These two statements, the lack of precision and the necessity of introducing a potential for inflation, are the main focus of this thesis and follow from a long history of different questions asked throughout humanity leading to our current understanding of the evolution of the Universe. How did Earth form? Where do the stars come from and where are they hung up? How did our Universe evolve? All those questions are asked in humanity for more than five thousand years now and are part of the field of cosmology. Cosmology (from Greek *kosmos* "world" and *-logia* "study of") deals with those questions and in more general with the origin and the evolution of our Universe from the Big Bang to today and on into the future.

First written records go back to Babylonian times (around 3000 BC) and describe the Earth and the Heavens forming a unit floating within infinite "water of chaos" [1]. Since the Babylonian times, our knowledge about the cosmos has grown tremendously and our description of the evolution of the Universe has changed a lot. A big step was the Copernican revolution, which led to the first heliocentric model, which assumes that the planets of our solar system orbit the Sun, so the Earth is not the center of our Universe. Johannes Kepler refined this model by including elliptical orbits to describe the trajectories of the planets in our solar system quite accurately. His calculations are still the basics for planetary motion. Although, he still fixed the stars on a celestial sphere. This celestial sphere was first associated to a physical model by Isaac Newton, who described the Universe to be filled with particles equally distributed which gravitationally attract each other and are in an unstable, but balanced circumstance. From this point on almost all models of our Universe described a static Universe. Only with the Theory of General Relativity the view of our Universe changed. Albert Einstein introduced the cosmological constant Λ to achieve a static Universe, in which Λ counteracts gravity, and Willem De Sitter proposed an expanding spatially flat Universe with a positive Λ . These two further led to different models with the original Big Bang model by Alexander Friedmann and Georges

Lemaître as the most noteworthy. This Big Bang model can describe the observations of Edwin Hubble and the calculations of Georges Lemaître showing that our Universe is expanding, as galaxies further away from us drift away faster, which is known as the Hubble-Lemaître law. The conclusion was that our Universe had a beginning, the Big Bang, a single initial high-density state ("primeval atom") that expanded. From the first Big Bang model evolved a class of models known as Friedmann-Lemaître-Robertson-Walker (FLRW) models, named in honour of Alexander Friedmann, Georges Lemaître, Howard Robertson and Arthur Walker. All models in this class obey the cosmological principle. The principle states that the Universe is spatially homogeneous and isotropic. This class of models, especially the Λ CDM (Cold Dark Matter), is known as the standard model of cosmology and is the best tested until today. The abbreviation Λ CDM indicates that all these models include a cosmological constant Λ , which functions as Dark Energy, and cold Dark Matter, i.e. there is a matter component present in the Universe which only interacts gravitationally with the visible matter. The cosmological constant is a possible solution and a requirement to explain the accelerated expansion of the Universe. The addition of Dark Matter in the Universe is the current explanation of velocity profiles of galaxies. According to classical mechanics, which is an accurate description of rotations of galaxies, the velocity of outer objects of galaxies should be lower than inner parts around the core. This decrease cannot be found from observations, but the velocity seems to be nearly constant over the galaxy. A solution to explain such a velocity profile is to include non-visible matter, which is arranged in a halo around the galaxy.

A question, which arises in the context of galaxies, is how the galaxies and the large scale structure, we see in the Universe, formed. Another important conclusion from observations is that our Universe is spatially flat, which very unlikely arises only from a Big Bang. A third conundrum thrown up by a basic Big Bang theory is how to explain the relative evenness of the temperature of the CMB. The question of structure formation, the flatness as well as the low temperature fluctuations of the CMB should be answered by a cosmological model, but the Λ CDM model class cannot explain structure formation, the flatness or the small temperature fluctuation. To explain all of those properties, in the 1980s Cosmic Inflation theory was developed, with notable contributions by several theoretical physicists, including Alexei Starobinsky, Alan Guth and Andrei Linde. Cosmic inflation is the idea that the very early Universe went through an era of accelerated expansion during the first 10^{-35} s before settling down to the more sedate rate of expansion we are still observing, so that all of the observable Universe originated in a small causally-connected region, which might be an explanation for the small temperature fluctuations of the CMB. Although, the Universe has been expanding since the initial Big Bang, inflation refers to the hypothesis that, for a small fraction of a sec-

ond, the Universe expanded suddenly, rather than the much slower and gradual expansion it followed since inflation, except the recent accelerated expansion. Guth hypothesized that the observable Universe is only a very small part of the actual Universe. In fact, Guth's calculations suggest that the entire Universe may be at least 10^{23} times bigger than the observable Universe [2]. An imprint of inflation is the large-scale structure of the CMB, which is a black body radiation and the earliest image of the Universe we are observing. The spectrum of the CMB can be related to a spectrum of quantum fluctuations during inflation. A small change in the duration of inflation can have a huge impact on predictions of the shape of the power spectrum and, therefore, it is important to study the duration of inflation precisely. It is still not clear what triggered the inflationary epoch, the best guess is a scalar field dominant in the Universe, which leads to a finite vacuum energy density and, therefore, can provide an accelerated expansion. With inflation being the latest addition to the cosmological models, it rounds up the look back into the history of cosmology.

In this thesis, I first introduce the standard model of cosmology, the Λ CDM model, defined by its line element. The important fundamental force for the evolution of the Universe is gravity, therefore, I use the theory of General Relativity to derive the equations of motion, the Friedmann equations, which describe how the Universe evolves. In the context of the Λ CDM model, I also mention the composition of the Universe and derive some thermodynamic quantities, which will become helpful for later calculations. The introduction of Λ CDM is completed by the definition of redshift, which is a main measurement parameter in astronomic observations and for cosmological studies. With the cosmological model in hand, I discuss the latest space-based observation of the CMB, done by the Planck satellite and some results of this mission. From this observation, one can see the different weaknesses mentioned earlier. Furthermore, I give the basic idea of inflation and the slow-roll paradigm. Due to the fact, that the duration or the amount of inflation is important, I describe how one can parametrize this amount, given by the number of e-folds. Inflation was introduced to solve some of the weaknesses of the Λ CDM model, therefore, I will demonstrate, how inflation can solve those weaknesses. The end of this introduction of the Λ CDM model and cosmic inflation is a brief thermal history of our Universe according to the current state of research and completes Chapter 2. The whole introduction up to this point has already been done by other physicists and can be found in literature. With the observation already mentioned, I investigate how to improve the precision of the analysis method of the Planck collaboration, which is the first statement and topic of my thesis. Therefore, I will derive the equation which connects an inflation model with the number of e-folds, used by the Planck collaboration to test different inflationary models and derive this equation step by step. As observational methods improve,

the measurements of different parameters become better as well. Thus, it may be possible to measure new effects, which have not been considered in the current analysis methods. To consider those additional effects, I investigate how those effects appear in the equation and add the needed terms. The theoretical background to derive the equation and add these effects is given in Chapter 2, whereas the inclusion of these effects is the content of Chapter 3. In the last part of my thesis, Chapter 4, I introduce a new approach to combine the duration of inflation and the parameters of the primordial power spectrum without the necessity to choose a potential for the inflation model. This new approach can be an additional cross check for testing models of inflation. Therefore, I use the horizon-flow parameters, which is an alternative to parametrizing the slow-roll regime of inflation (The slow-roll parametrization is described in Chapter 2.3.1). I show that this new approach is able to predict how the parameters of the primordial power spectrum evolve under a change of the duration of inflation. To calculate the behaviour, the predicted measurement errors for those parameters for future experiments are used as well as the best fit values from the Planck satellite.

From Big Bang to galaxy structures

2

This chapter deals with basic properties of the Λ CDM model. It summarizes important aspects of thermodynamics to describe an expanding universe. We introduce some of the current measurements and show where the standard model of cosmology performs well and where its weaknesses are. As a solution to some of those weaknesses, we introduce and discuss cosmic inflation as an extension to Λ CDM. We briefly have a look at how large scale structure forms by including inflation and finish with a summary of the thermal history of our Universe.

2.1 Λ CDM - Standard model of cosmology

For the evolution of our Universe gravity is the most important fundamental force. Therefore, we want to have a description which is consistent with Einstein's theory of General Relativity and its field equations. The mathematical description should also include the cosmological principle, i.e. the Universe is spatially homogeneous and isotropic. A line element which obeys all those conditions is the Friedmann-Lemaître-Robertson-Walker (FLRW) line element,

$$ds^2 = -dt^2 + a^2(t) \left(\frac{dr^2}{1-kr^2} + r^2(d\theta^2 + \sin\theta d\phi^2) \right), \quad (2.1)$$

where we utilized spatial spherical coordinates (r, θ, ϕ) and cosmic time t . The scale factor $a(t)$ is appearing, as well as the curvature parameter k , which is -1 for a hyperbolic space, $+1$ for a spherical space and 0 for an Euclidean space. To describe the expansion of the Universe, we have to find the equations of motion. Therefore, we use the Einstein field equations,

$$R_{\mu\nu} - \frac{1}{2}g_{\mu\nu}R + \Lambda g_{\mu\nu} = 8\pi G T_{\mu\nu}, \quad (2.2)$$

where $R_{\mu\nu}$ is the Ricci Tensor, R the Ricci scalar, Λ the cosmological constant, G Newton's gravitation constant and $T_{\mu\nu}$ the energy-momentum tensor. From the line element Eq. (2.1) we can calculate all Christoffel symbols and from those the Riemann tensor, Ricci tensor and

Ricci scalar. For the energy-momentum tensor we use the one of a perfect fluid,

$$T^{\mu\nu} = Pg^{\mu\nu} + (\rho + P)u^\mu u^\nu, \quad (2.3)$$

where P is the pressure of the fluid, ρ the energy density and u^μ the four-velocity. Evaluating the time-time component of the Einstein equations leads to

$$H^2 + \frac{k}{a^2} = \frac{8\pi G}{3}\rho + \frac{\Lambda}{3}, \quad (2.4)$$

which is the first Friedmann equation, where H is the Hubble rate defined as $H = \dot{a}/a$. While the first Friedmann equation arises from the time-time component of Eq. (2.2), the second Friedmann equation follows from the diagonal space-space components,

$$-\left(2\dot{H} + 3H^2 + \frac{k}{a^2}\right) = 8\pi GP - \Lambda. \quad (2.5)$$

Usually, instead of the second Friedmann equation the energy-momentum conservation is used,

$$\dot{\rho} + 3H(\rho + P) = 0. \quad (2.6)$$

The Eqs. (2.4) and (2.6) together with the definition of H and the equation of state $P = P(\rho)$ form a closed set of equations and describe the evolution of a homogeneous and isotropic Universe. ρ receives contributions from all forms of energy in the Universe including relativistic matter called "radiation" and non-relativistic matter or dust just called "matter". Often, energy densities for curvature and the cosmological constant or Dark Energy are defined as well,

$$\rho_{\text{curv}} \equiv -\frac{k}{a^2} \frac{3}{8\pi G}, \quad \rho_\Lambda \equiv \frac{\Lambda}{8\pi G}. \quad (2.7)$$

Considering now the simplest case for the equation of state, namely $w = P/\rho = \text{const.}$, we can solve the energy-momentum conservation law (2.6) for ρ to find

$$\rho = \rho_0 \left(\frac{a_0}{a} \right)^{3(1+w)}. \quad (2.8)$$

With this relation, we can describe how the scale factor evolves in time for each component of energy in the Universe. Considering an arbitrary w with the condition $w > -1$ and plugging the solution for ρ into the first Friedmann equation (2.4) yields the solution for the scale factor as a function of cosmic time [3]

$$a \sim t^\alpha \quad : \quad w > -1 \quad \text{with} \quad \alpha = \frac{2}{3} \frac{1}{1+w}, \quad (2.9)$$

where we only consider the case $k = 0$. We can insert the equation of state for dust and radiation, whereas for Dark Energy, with $w = -1$, we have to derive the relation between scale factor and time directly from the Eq. (2.4),

$$a \sim t^{2/3} : w = 0 \quad (\text{dust/non-relativistic matter}), \quad (2.10)$$

$$a \sim t^{1/2} : w = \frac{1}{3} \quad (\text{radiation/relativistic matter}), \quad (2.11)$$

$$a \sim \exp(Ht) : w = -1 \quad (\text{cosmological constant/Dark Energy}). \quad (2.12)$$

For radiation we can calculate the energy density as a function of temperature. This helps us to see which particles are part of radiation at a certain time during the evolution of the Universe, as done in a similar way in [4]. Therefore, we neglect interactions and assume that there are equal amounts of particles and antiparticles of a species of fermions or bosons. Considering now an infinitesimal volume of phase space for this particle species with momenta between p and $p + dp$, the number of particles in this volume element is

$$dN = \frac{g_i}{(2\pi)^3} f_{\pm}(p, T) dV dp \quad (2.13)$$

with g_i the internal degrees of freedom of the specific particle species and

$$f_{\pm}(p, T) = \frac{1}{e^{E(p)/T} \pm 1} \quad (2.14)$$

the distribution function of either fermions, given by the plus sign, or bosons, given by the minus sign, where $E(p)$ is the energy. Multiplying the number of particles with their energies and integrating over all momenta provides us with the energy density

$$\rho_i(T) = \int \frac{d^3 p}{(2\pi)^3} E(p) g_i f_{\pm}(p, T). \quad (2.15)$$

By including spherical coordinates in phase space and with the relativistic dispersion relation $E(p) = \sqrt{p^2 + m_i^2}$, we can rewrite the integral as

$$\rho_i(T) = g_i \int \frac{dp}{2\pi^2} p^2 \sqrt{p^2 + m_i^2} f_{\pm}(p, T). \quad (2.16)$$

Considering the ultra-relativistic limit ($m = 0, p = E$), we can calculate the integral,

$$\rho_i(T) = \frac{g_i T^4}{2\pi^2} \int_0^\infty dx \frac{x^3}{e^x - 1} = g_i T^4 \frac{1}{2\pi^2} \zeta(4) \Gamma(4) = \frac{\pi^2}{30} g_i T^4, \quad (2.17)$$

with the substitution $x = E/T$, ζ the Zeta-function and Γ the Gamma-function. This result only holds for bosons, for fermions we have to use the distribution function with a plus sign

and the overall result is modified by a factor of $7/8$. In general, the degrees of freedom are also temperature dependent and we can find the relation between temperature and degrees of freedom by substituting $p \rightarrow E$ in Eq. (2.16) and normalizing by the result from Eq. (2.17),

$$\frac{\rho_i(T)}{\frac{\pi^2}{30} T^4} = g_i \frac{15}{\pi^4} \int_{m_i/T}^{\infty} dE E^2 \sqrt{E^2 - \left(\frac{m_i}{T}\right)^2} f_{\pm}(E) = g_{i,\text{eff}}(T). \quad (2.18)$$

The overall degrees of freedom are the sum over all individual degrees of freedom for each particle species,

$$g_{\text{eff}} = \sum_i g_{i,\text{eff}} = g_{\text{eff}}(\gamma) + g_{\text{eff}}(\nu) + g_{\text{eff}}(e) + g_{\text{eff}}(\mu) + \dots = 2 + \frac{7}{8} 2N_{\text{eff}} + g_{\text{eff}}(e) + g_{\text{eff}}(\mu) + \dots, \quad (2.19)$$

where N_{eff} is the number of flavours of neutrinos, which in the case of massless neutrinos, like in the standard model of particle physics, is $N_{\text{eff}} = 3$. This relation can now be used to compute the effective degrees of freedom, allowing to see at which temperature which particles contribute to the energy density of radiation. Hence, we consider all particles relevant during the evolution of the Universe (compare Tab. 2.1), which are mainly the particles of the standard model of particle physics and the pions. Plotting the effective degrees of freedom as a function of temperature given by Eq. (2.18) for all particles shown in Tab. 2.1 leads to Fig. 2.1. The threshold for each particle that becomes relativistic is defined by a temperature equal to a third of the mass of the particle. This assumption can be made, because the average kinetic energy of a particle in a gas is $\bar{E} \sim 3k_B T$ and we demand this kinetic energy is roughly of the same order as the rest energy to state that a particle is relativistic.

After investigating the calculation of the energy density of radiation in more detail, we also inspect another important thermodynamic property characterising a system which is entropy. The detailed derivation can be found in [3]. In thermodynamics, the entropy appears in the first law, which can be written for the general case of varying particle numbers,

$$dE = TdS - PdV + \sum_i \mu_i dN_i, \quad (2.20)$$

where the index i labels once again particle species, S is the total entropy of the system and μ_i is the chemical potential of a particle species. Both, energy E and the number of particles N , are extensive quantities, i.e. they scale with the volume of the system, while temperature and pressure are local quantities. That is why according to the first law (2.20), entropy is also an extensive quantity. As we already discussed the energy density for radiation, it is convenient to introduce the entropy density s and the number density n ,

$$s \equiv \frac{S}{V}, \quad n = \frac{N}{V}. \quad (2.21)$$

	m/MeV	F or B	g_i
γ	0	B	2
ν	0	F	6
u	2.4	F	12
d	4.8	F	12
s	95	F	12
c	1275	F	12
b	4200	F	12
t	177000	F	12
g	0	B	16
e	0.5	F	4
μ	106	F	4
τ	1700	F	4
W	80300	B	6
Z	91100	B	3
H	125300	B	1
π^0	135	B	1
π^\pm	139	B	2

Table 2.1: Used particles for the calculation of the degrees of freedom as a function of temperature during the evolution of the Universe, where m/MeV is the mass of a particle in MeV and g_i are the spin degrees of freedom [5]. The column for F or B denotes if the particle is either a fermion (F) or a boson (B).

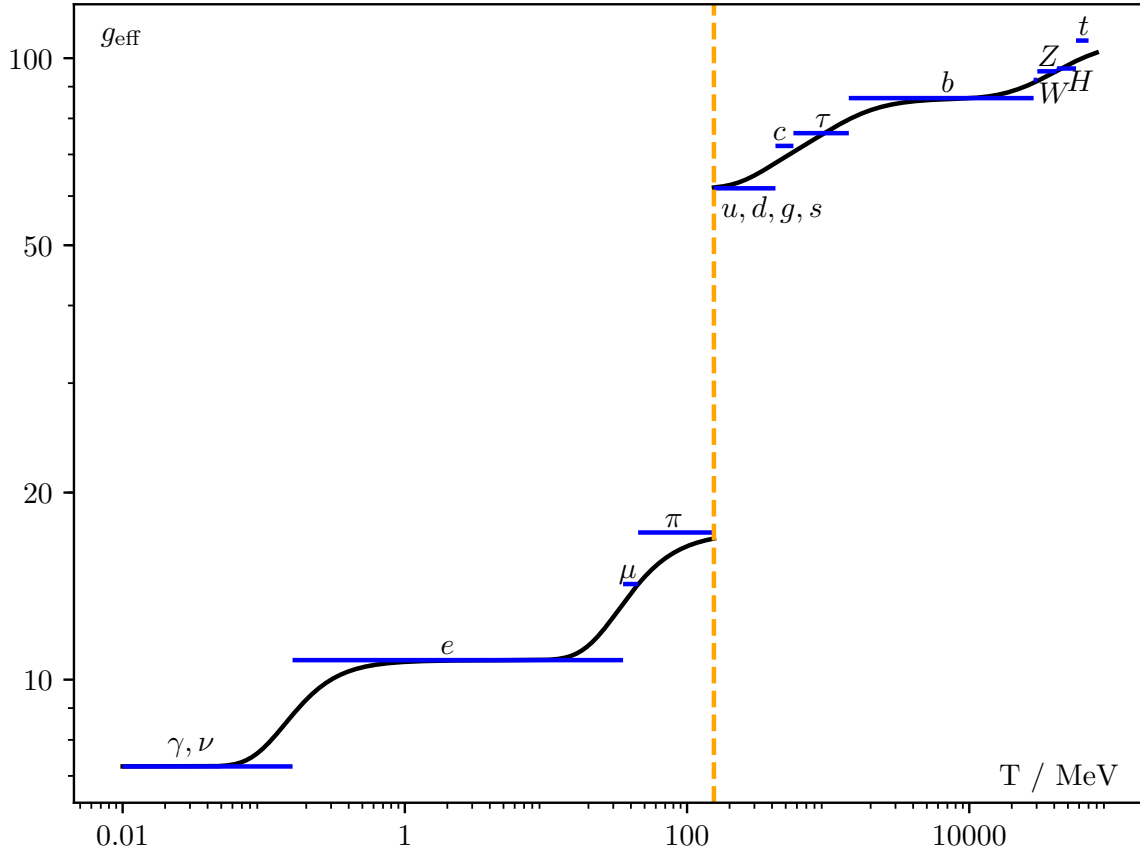


Fig. 2.1. Effective degrees of freedom as a function of temperature. The dashed line is the quantum chromodynamics crossover at $T = 155$ MeV. The blue lines are Heaviside functions for each particle type, and the black line is the continuous one using Eq. (2.18). Masses and degrees of freedom are taken from Tab. 2.1.

We now rewrite the first law of thermodynamics by inserting those densities,

$$(Ts - P - \rho + \mu n)dV + (Tds - d\rho + \mu dn)V = 0, \quad (2.22)$$

and consider a region of constant volume, which can be realised in an expanding universe by using the comoving volume, yielding

$$Tds = d\rho - \mu dn. \quad (2.23)$$

By using Eq. (2.22) and considering the whole volume, we find the entropy density

$$s = \frac{P + \rho - \mu n}{T}. \quad (2.24)$$

We now consider again radiation and include the assumption of equal numbers of particles and antiparticles which was used to derive the energy density. This assumption leads to a vanishing chemical potential and the entropy density simplifies to

$$s = \frac{P + \rho}{T}. \quad (2.25)$$

Making use of the equation of state for radiation and the energy density for a specific particle species, we find an expression for the contribution for a particle species to the entropy density

$$s_i = \frac{4 \rho_i}{3 T} = \begin{cases} h_i \frac{2\pi^2}{45} T^3 & - \text{bosons} \\ \frac{7}{8} h_i \frac{2\pi^2}{45} T^3 & - \text{fermions} \end{cases}, \quad (2.26)$$

where h_i are the effective degrees of freedom for the entropy density, which can be different to those degrees of freedom g_i appearing in the energy density. Besides the fact that entropy is a characteristic property of a thermodynamic system such as the Universe, we can utilize another property which will be one of, if not the most, important fact in the later calculation of this thesis. Therefore, we examine the second law of thermodynamics which tells us that the entropy of any closed system can only increase, and it stays constant for an equilibrium evolution, i.e. smooth evolution during which the system always stays in thermal equilibrium, called adiabatic evolution. Coming back to the relation in Eq. (2.20), instead of using the number of particles we use the related quantum numbers which are also connected to chemical potentials. We apply the relation to a comoving volume $V = a^3$ in the Universe. Due to the fact that quantum numbers are a conserved quantity in a comoving volume and energy conservation is given by Eq. (2.6), we find

$$T \frac{dS}{dt} \equiv T \frac{d(sa^3)}{dt} = (P + \rho) \frac{dV}{dt} + V \frac{d\rho}{dt} = a^3 \left((P + \rho) \cdot 3 \frac{\dot{a}}{a} + \dot{\rho} \right) = 0. \quad (2.27)$$

From this equation we conclude that the total entropy in a comoving volume is conserved,

$$sa^3 = \text{const.} \quad (2.28)$$

After this excursion into the thermodynamics of the Universe, let us investigate the cosmic time a little bit more. Since observations measure the redshift of an object, which is drifting away from us due to the cosmic expansion, and not the cosmic time, it is convenient to rewrite the Friedmann equations in terms of redshift. The definition of redshift is the difference in frequency between the emitter E and the observer 0 normalized by the observed frequency,

$$z \equiv \frac{\nu_E - \nu_0}{\nu_0}. \quad (2.29)$$

As light is our main observable and it travels along a null geodesic, i.e. $ds^2 = 0$, we find the relation $dt = -a dr$, where we chose the negative sign such that the light ray is incoming. Dividing $dt = -a dr$ by a and integrating both sides from the source to the observer yields

$$\int_{t_e}^{t_0} dt \frac{1}{a(t)} = - \int_{r_{\text{source}}}^{r_{\text{observer}}} dr. \quad (2.30)$$

The right-hand side is independent of the observation and emission times, so the left-hand side has to be constant. Consequently, the integral boundaries on the left-hand side can be shifted by Δt_e , respectively Δt_0 . Comparing the difference between the original and the shifted integral for small Δt yields the equation $\Delta t_0/a_0 = \Delta t_e/a_e$. Since $v_0/v_e = \Delta t_e/\Delta t_0$, the redshift can be expressed by the scale factor,

$$1 + z(t) = \frac{a_0}{a(t)}. \quad (2.31)$$

Interestingly, for small velocities and, therefore, small redshifts the redshift equals approximately the velocities. Furthermore, $a_0/a(t)$ can be expanded to

$$\frac{a_0}{a(t)} \approx 1 + \frac{\dot{a}_0}{a_0}(t_0 - t) = 1 + H_0(t_0 - t), \quad (2.32)$$

where $H_0 = H(t_0)$ is the Hubble parameter. For small time differences, we have $\delta t \approx adr$. Combining all this results in the Hubble-Lemaître law

$$v \approx H_0 r, \quad (2.33)$$

i.e. that all objects in our Universe move apart from every point with a velocity which is proportional to the distance between the object and that point. This can be observed today.

For more convenience, we introduce as a last step density parameters Ω_i where i denotes a specific sort of energy which appears in the energy density ρ in Eq. (2.4). These density parameters are,

$$\Omega_i \equiv \frac{\rho_i}{\rho_c} = \frac{\rho_i}{\frac{3}{8\pi G}H_0^2}, \quad (2.34)$$

where i is either radiation (relativistic matter), matter (combining Dark Matter with baryonic matter), curvature or the cosmological constant.

With all these ingredients, we can rewrite the first Friedmann equation (2.4) in the convenient form,

$$H^2 = H_0^2 \left[\Omega_R(1+z)^4 + \Omega_m(1+z)^3 + \Omega_k(1+z)^2 + \Omega_\Lambda \right], \quad (2.35)$$

where all Ω_i are evaluated today. All models containing a cosmological constant Λ and cold Dark Matter, i.e. Dark Matter which is non-relativistic, and using the Friedmann-Lemaître-Robertson-Walker metric, the Friedmann equation and the simple form of the equation of state ($P = w\rho$) are called Λ CDM-models.

2.2 Observations - Studying the Universe experimentally

With the theoretical framework established let us do some observations to see if our assumptions are valid or not. Therefore, we observe a background radiation present in the whole Universe, the CMB. This remnant of the Big Bang arose from the time of recombination, an epoch we will discuss in a later stage. It was first detected by Arno Penzias and Robert Woodrow Wilson in 1964 as they tested a new sensitive antenna [6]. In 1978 Penzias and Wilson were awarded with the Nobel Prize in physics.

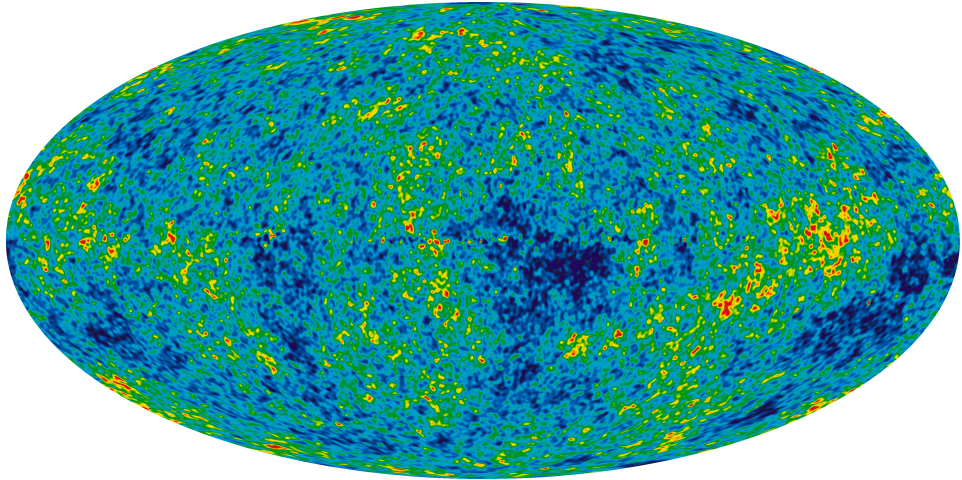


Fig. 2.2. Image of the CMB observed by the Wilkinson Microwave Anisotropy Probe (WMAP). All-sky picture of the infant Universe created from the WMAP data [7]. The different colour scheme shows temperature fluctuations of $\pm 200 \mu\text{K}$.

The CMB is a near perfect black body radiation arriving from all around the Universe (see Fig. 2.2). Black body radiation has the property of a well determined power spectrum \mathcal{P} and can be associated with a radiation temperature which is (2.7255 ± 0.0005) K [8] for the CMB.

As the CMB is the earliest image of the Universe, it is predestined to be observed and provide the data with which cosmological models can be tested, because it allows us the furthest look back into the Universe. Therefore, a lot of experiments, ground based as well as space based were done. The latest space based one being the Planck satellite [9]. The Planck

satellite was an all sky survey operating in a range from 27 GHz up to 857 GHz, which was launched in May 2009 and run until October 2013. It observed the whole CMB for roughly four years with the latest data being released in 2018, which also included the power spectrum. As the CMB from all over the Universe and can be treated as a sphere around us, it is possible

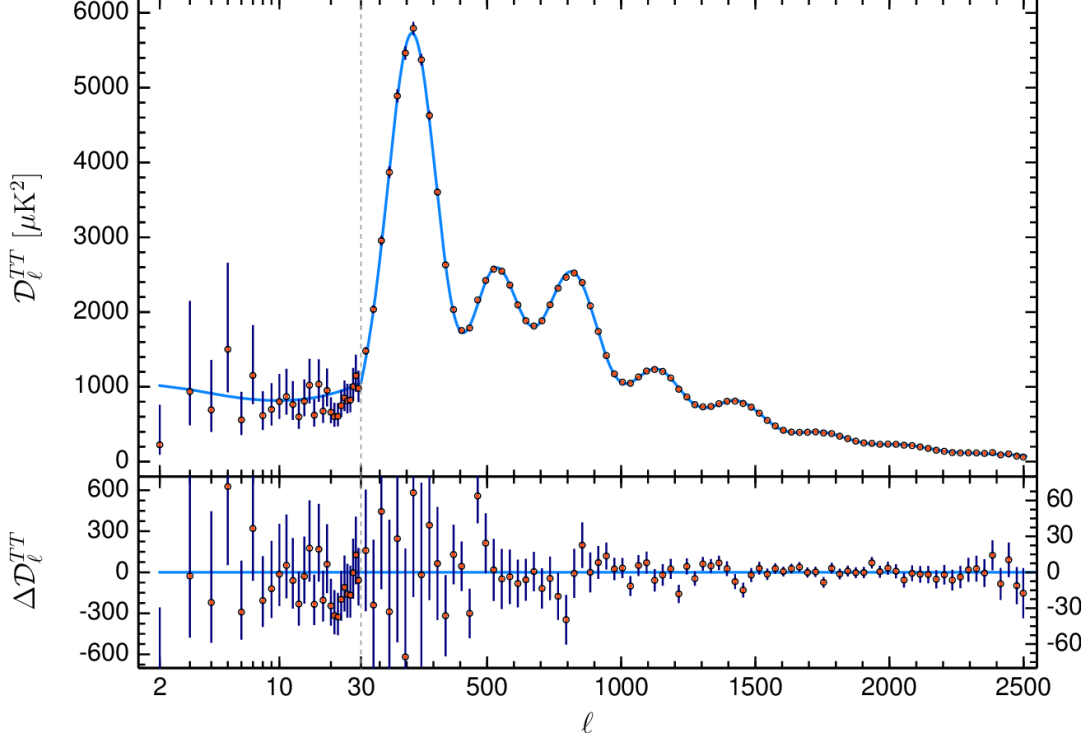


Fig. 2.3. Power spectrum of the CMB in terms of multipoles of the structures observed [10]. The red dots represent the measurements from Planck with a 1σ errorbar in purple. The blue line is the theoretical spectrum predicted by the Λ CDM model.

to expand its power spectrum into spherical harmonics and write as

$$T(n) = \sum_{l=0}^{l_{\max}} \sum_{m=-l}^l a_{lm} Y_{lm}(n), \quad (2.36)$$

where Y_{lm} are the spherical harmonic functions and the coefficients are

$$a_{lm} = \int_{4\pi} T(n) Y_{lm}^*(n) d\Omega, \quad (2.37)$$

where the star denotes the complex conjugation operation. With these expressions, we can express the CMB as an angular power spectrum which measures the amplitude as a function of wavelength. Accordingly the definition of the amplitude of different multipole moments is

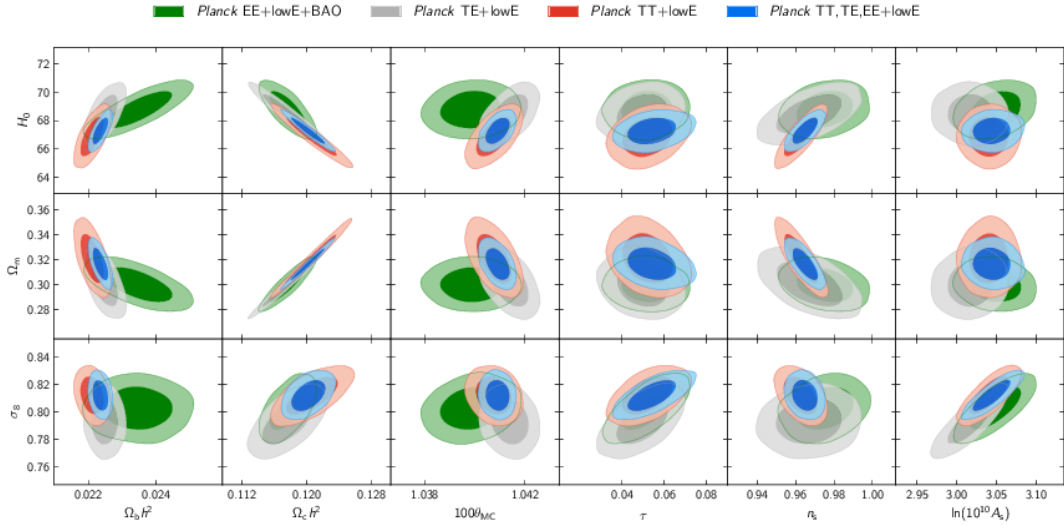


Fig. 2.4. Correlation between the six parameters necessary to test Λ CDM and the three derived parameters Ω_m , H_0 and σ_8 [10]. Different colours represent different analysed data sets.

$$C_l = \frac{1}{2l+1} \sum_{m=-l}^l |a_{lm}|^2. \quad (2.38)$$

The usual procedure is to plot $D_l \equiv l(l+1)C_l/(2\pi)$ instead of C_l , which was used in Fig. 2.3.

Besides the power spectrum, we also need some observable cosmological parameters to test if our model predicts those parameters in accordance with the observation. To test the Λ CDM model, six parameters are needed. From the CMB we can get those six independent parameters, which are $\Omega_b h^2$, $\Omega_c h^2$, $100\theta_{MC}$, τ , n_s and $\ln(10^{10} A_s)$. Ω_b is the density parameter for baryonic (visible) matter in the Universe, where h is the factor of the Hubble rate defined by $H_0 = h \cdot 100 \text{km}/(\text{s}\cdot\text{Mpc})$. The density parameter Ω_c is the contribution from cold Dark Matter. The parameter $100\theta_{MC}$ denotes the scale of baryon acoustic oscillations times 100 appearing in the CMB. Those oscillations arise from fluctuations in the density of the visible matter caused by acoustic density waves in the primordial plasma of the early Universe. The fourth parameter τ is the optical depth of the Universe giving information about how transparent the Universe is. As we mentioned, the power spectrum we can measure has two important parameters, which are the last two parameters, but these are not the parameters of the power spectrum we observe today. Instead, it is the primordial power spectrum of perturbations leading up to the large scale structure imprinted in the CMB. The spectral index n_s gives the slope of the primordial power spectrum, where the parameter A_s is the amplitude of those primordial fluctuations. These six parameters can then be fitted to the Λ CDM model.

From the Planck data it is also possible to extract more cosmological parameters. For example, in our derivation previously done, we used Ω_m instead of the separation into different components of matter and the Hubble rate appears in the first Friedmann equation as well. Those parameters can be derived but with an error attached to them (see Fig. 2.4).

The parameters themselves have also some cross-correlations, which influences the value of them and leads to an error depending on different data sets used. We will use some of those parameters in the later stages of this thesis and it is important to remember that those errors exist and have to be taken into account as we perform calculations. The cross-correlations can be found in Fig. 2.5, where also the Hubble parameter is added, which is a derived quantity.

With the observations done we get values for the different density parameters and some other cosmological parameters [10],

$$\Omega_m = 0.321 \pm 0.013, \quad \Omega_\Lambda = 0.679 \pm 0.013, \quad \Omega_k = 0.0007 \pm 0.0019, \quad (2.39)$$

with a 68% confidence level. Also, we find that the Hubble rate of today H_0 is $(66.88 \pm 0.92) \text{ km s}^{-1} \text{ Mpc}^{-1}$ and we can reconstruct the age of Universe to be $(13.830 \pm 0.037) \text{ Gyr}$. Dark Matter can be stated to be cold, as we measure no other signature than the gravitational one. All spatially flat cosmological models with Dark Energy and cold Dark Matter, using parameters close to Eq. (2.39), are called flat Λ CDM models.

Another important feature about the CMB is that the temperature fluctuations are four orders of magnitude smaller than the mean temperature, i.e. the primordial perturbations, which led to the CMB structure, have been in thermal equilibrium and, therefore, causally connected. The CMB formed during the time of recombination. When first atoms formed, the Universe became transparent and photons could stream freely. Those free streaming photons are the CMB. The temperature of recombination can be calculated¹ and is roughly 0.3 eV, which corresponds to a redshift of $z_{\text{re}} \approx 1100$. With the redshift of recombination, we can use the assumption of Hubble expansion and reconstruct the causally connected parts of the CMB, which should be the whole CMB or at least a large part of it to explain the small temperature fluctuations and be consistent with the age of the Universe. Therefore, we can calculate the Hubble scale at recombination, which is 0.47 degrees. The exact formula is $0.86 \Omega_m \text{ deg}$ [11]. So, the Λ CDM model suggests that the CMB was not causally connected as a whole and, therefore, can not explain, why the CMB has such small temperature fluctuations. This circumstance is known as the horizon problem.

Another problem is galaxy formation. We started with the cosmological principle and have investigated the expansion of our Universe as a perfect fluid. Inhomogeneities are not taken

¹For the interested reader a detailed calculation can be found in Chapter 6 of [3].

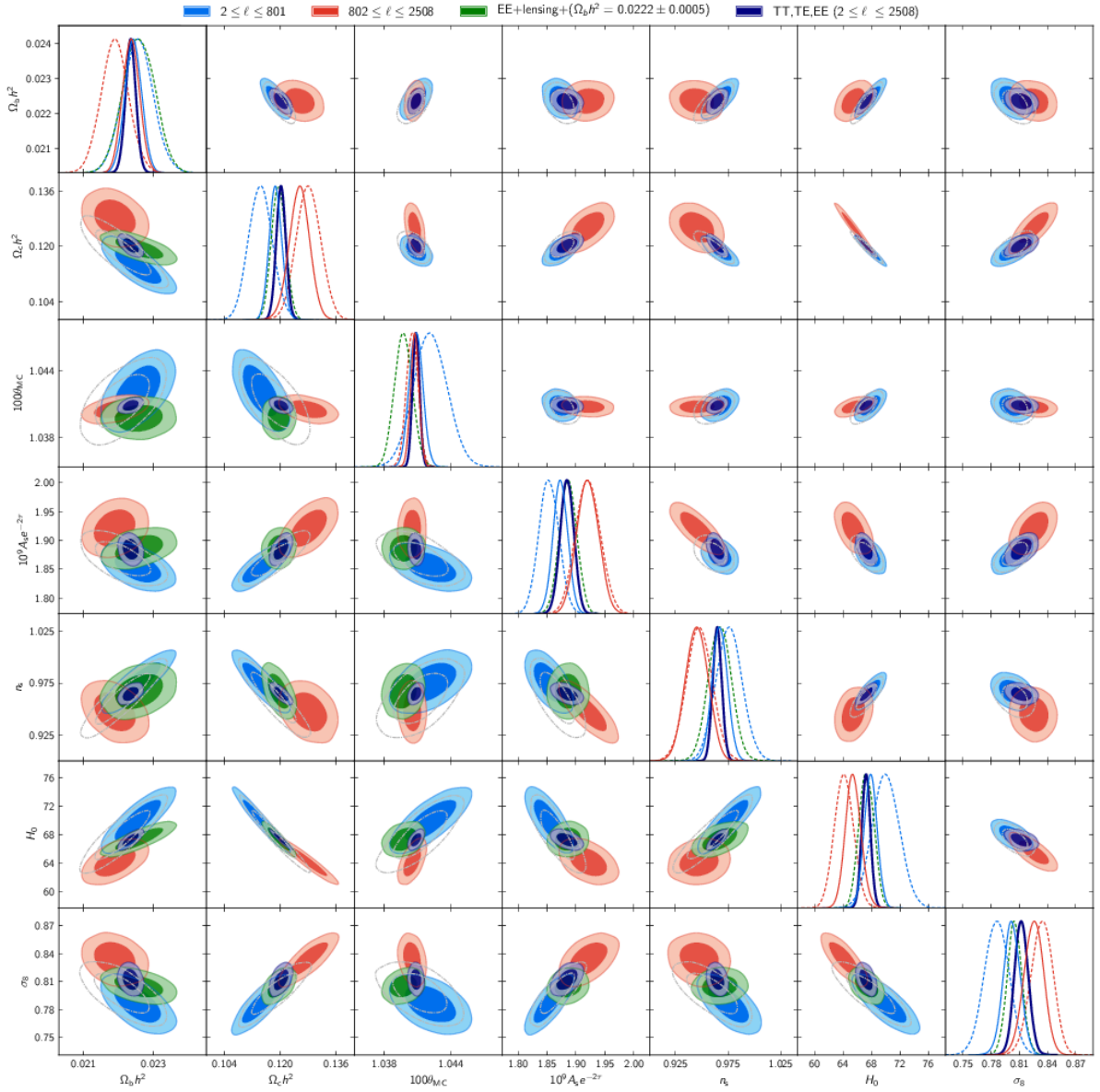


Fig. 2.5. Base- Λ CDM 68% and 95% parameter constraint contours from the CMB power spectrum [10]. The different segments represent the entry of the covariance matrix which indicates how related those two parameters are. The different colour coding represents different data sets.

into account in this theory by definition, but we observe highly inhomogeneous structures in the Universe at scales less than 200 Mpc. Those inhomogeneities are galaxies, galaxy clusters and super clusters with raising density towards the inner regions of those objects. To generate those structures, we need some process which is not incorporated into the Λ CDM model.

A third curiosity in the context of Λ CDM and the observations of the CMB is the small amount of curvature our Universe has. To be more precise, our Universe is nearly spatially flat. This circumstance is hard to explain by such an inhomogeneous explosion as the Big Bang. The probability for the fine tuning of initial conditions to achieve a universe with that flatness our Universe has is very unlikely. This is another weakness of the Λ CDM model and known as the flatness problem.

All those weaknesses described above need some solutions and, therefore, either a new model or an extension to the Λ CDM model is required. One possible candidate is cosmic inflation, which is currently the most researched one.

2.3 Cosmological inflation - Seeds for structure formation

The weaknesses of Big Bang models were already known in the mid 20th century. In 1980, Alan Guth published an idea inspired by particle physics which adds an epoch of rapid expansion shortly after the Big Bang and is called inflation [2]. In his work, he used inflation as a solution to the horizon and flatness problem. Furthermore, we will investigate how we can explain structure formation with inflation.

The definition of inflation is rather simple,

$$\text{inflation} \Leftrightarrow \ddot{a} > 0. \quad (2.40)$$

Each epoch in which this condition is satisfied is an inflationary epoch. Also, this condition has another consequence. If we insert $\ddot{a} > 0$ into the second Friedmann equation (2.5) and also use the first Friedmann equation (2.4), we get the equation of state for this epoch which is $p < -\rho/3$. Due to the construction of the Friedmann equations, this equation of state is the dominant one, so the physical components during an inflationary epoch have to obey it. This equation of state violates the strong energy condition and neither ordinary baryonic matter nor radiation satisfies $p < -\rho/3$. From quantum field theory we know a component which satisfies such an equation of state, namely a scalar field. Thus, we investigate that during inflation a scalar field or maybe multiple scalar fields are dominant. Such fields are called inflaton fields ϕ .

2.3.1 The inflaton field

Due to the large variety of possible combinations of scalar fields, we will stick to the simple case of a single scalar field during inflation. For this single field, we can write down the action considering minimal coupling to gravity,

$$S = \int d^4x \sqrt{-g} \mathcal{L} = \int d^4x \sqrt{-g} \left(\frac{1}{2} \partial_\mu \phi \partial^\mu \phi - V(\phi) \right), \quad (2.41)$$

where V is the potential of the scalar field and $\sqrt{-g}$ the determinant of the (pseudo-)metric tensor $g_{\mu\nu}$. Considering a homogeneous scalar field in the spatially flat Universe with the FLRW metric (2.1), the action yields the equation of motion,

$$\ddot{\phi} + 3H\dot{\phi} + V'(\phi) = 0, \quad (2.42)$$

where the prime denotes a derivative with respect to the inflaton field ϕ . By taking a closer look at the energy-momentum tensor, which is

$$T_{\mu\nu} = \frac{2}{\sqrt{-g}} \frac{\delta S}{\delta g^{\mu\nu}} = \partial_\mu \phi \partial_\nu \phi - g_{\mu\nu} \mathcal{L}, \quad (2.43)$$

we find the energy density and the pressure as

$$\rho = \frac{1}{2} \dot{\phi}^2 + V(\phi), \quad (2.44)$$

$$p = \frac{1}{2} \dot{\phi}^2 - V(\phi). \quad (2.45)$$

For the case of inflation, the first Friedmann equation (2.4) becomes

$$H^2 = \frac{1}{3M_{\text{PL}}^2} \left(\frac{1}{2} \dot{\phi}^2 + V(\phi) \right), \quad (2.46)$$

where $M_{\text{PL}} = 1/\sqrt{8\pi G}$ is the reduced Planck mass.

One major feature worth mentioning here is that the potential V of the field is generally of free choice. Early inflation models used potentials which had a false minimum and the duration of inflation was determined by the tunnelling probability. Such models are known as 'old inflation'. This idea of a false minimum leads to the fact that the field tunnels into the true minimum differently at different locations and, therefore, domains develop. If two of those domains collide, a relic is formed which should be observable. Usually, such relics are gravitational waves, but it is also possible that those domains leave an imprint on the CMB or form monopoles, but nothing has been found yet. To avoid such developing of domains Andrei D. Linde [12] and, independently, Andreas Albrecht and Paul Steinhardt [13] presented

a solution to the domain wall problem by introducing the idea that the inflaton field has a smooth potential, but rolls down slowly to the minimum, which is why such models are called slow-roll inflation. This idea still provides an exponential expansion, but does not introduce any domains of different states. The regime of slow-roll occurs when the term $3H\dot{\phi}$, which is called Hubble friction term, dominates over the acceleration term in Eq. (2.42), i.e.,

$$\left| \frac{\ddot{\phi}}{3H\dot{\phi}} \right| \ll 1. \quad (2.47)$$

A second slow-roll condition ensures that the potential term is large compared to the kinetic energy in Eq. (2.46),

$$\frac{\dot{\phi}^2}{2V(\phi)} \ll 1. \quad (2.48)$$

Once these two conditions hold, we can rewrite Eqs. (2.42) and (2.46),

$$\dot{\phi} = -\frac{1}{3H}V'(\phi), \quad (2.49)$$

$$H = \frac{1}{M_{\text{PL}}} \sqrt{\frac{V}{3}}. \quad (2.50)$$

From the two conditions (2.47) and (2.48) and the new equation of motion (2.49), as well as the Friedmann equation during slow-roll inflation (2.50), we can define the slow-roll parameters

$$\varepsilon \equiv -\frac{\dot{H}}{H^2}, \quad (2.51)$$

$$\eta \equiv \varepsilon - \frac{\ddot{\phi}}{H\dot{\phi}}. \quad (2.52)$$

As long as $\varepsilon \ll 1$ and $\eta \ll 1$, slow-roll inflation takes place and in most inflationary models inflation ends when one of those parameters gets close to 1.

2.3.2 The number of e-folds

From the definition of H and Eq. (2.50), we derive the dependence of the scale factor $a(t)$ as a function of time in the slow-roll regime,

$$a(t) = a_i \exp \left(\int_{t_i}^t dt' H(t') \right) = a_i \exp \left(\sqrt{\frac{1}{3M_{\text{PL}}^2}} \int_{t_i}^t dt' \sqrt{V(\phi(t'))} \right), \quad (2.53)$$

where a_i is the scale factor at beginning of inflation. If we want to compare two scale factors at different times, we can use Eq. (2.53) and, therefore, know the factor of expansion of the

Universe in one direction. Usually, one wants to know the expansion from a given value of the field ϕ until the end of inflation. For this purpose, we define the number of e-folds \mathcal{N} from a time t_ϕ , when the field takes a certain value, to the end of inflation t_{end} ,

$$\mathcal{N}(\phi) \equiv \ln \left(\frac{a_{\text{end}}}{a(\phi)} \right) = \int_{t_\phi}^{t_{\text{end}}} dt H(t). \quad (2.54)$$

To resolve the flatness problem roughly 40 to 60 e-folds are required, but we discuss this in more detail in the next subsection.

2.3.3 Curing weaknesses of the Λ CDM-model

Now let us examine how that new epoch of inflation can help to solve some of the weaknesses of the Λ CDM model. Due to $\ddot{a} > 0$, the Universe expands faster and faster. This rapid expansion blows up the Universe by 20 to 30 orders of magnitude in one spatial direction, which happens roughly from 10^{-35} s to 10^{-33} s after the Big Bang. Only space expands during this time and the physical connected region stays roughly the same. Suppose inflation begins at t_i and that the Hubble rate stays constant throughout inflation, $a(t) = a_i \exp(H_{\text{inf}}(t - t_i))$. The comoving causal horizon during inflation is

$$d_p = \int_{t_i}^t \frac{dt}{a(t)} = \frac{1 - e^{-H_{\text{inf}}(t - t_i)}}{a_i H_{\text{inf}}} \simeq \frac{1}{a_i H_{\text{inf}}}. \quad (2.55)$$

If the comoving scale corresponding to the observable Universe today, $\lambda_0 \sim (a_0 H_0)^{-1}$ originates inside this causal horizon we conclude

$$\frac{\lambda_0}{d_p} < 1 \iff \frac{a_i H_i}{a_0 H_0} = \frac{a_i}{a_{\text{end}}} \frac{a_{\text{end}} H_{\text{inf}}}{a_0 H_0} = e^{-\mathcal{N}} \frac{a_{\text{end}} H_{\text{inf}}}{a_0 H_0} < 1, \quad (2.56)$$

where we used the definition of the number of e-folds (2.54). Rearranging yields

$$\mathcal{N} > \ln \left(\frac{a_{\text{end}} H_{\text{inf}}}{a_0 H_0} \right). \quad (2.57)$$

Since $H_0 \sim 10^{-42}$ GeV, if for example the scale of inflation is $H_{\text{inf}} \sim 10^{14}$ GeV this amounts to about $\mathcal{N} > 64$. This short calculation is also used in an advanced way to constrain inflation from observations, which we also investigate in more detail in Chapter 3. It can be concluded, inflation provides that the observable Universe and the CMB we see today were physically connected shortly after the Big Bang, which explains the low temperature fluctuations and resolves the horizon problem.

A similar explanation can be used to resolve the flatness problem. We do not know much about the Big Bang and how inhomogeneous it was, but due to the rapid expansion our observable Universe is only a small patch, which is locally flat, of the whole maybe highly curved Universe. One can imagine this circumstance like a tiny patch of a large sphere which for a local observer is nearly flat, whereas the whole sphere is highly curved. To add some calculations to this vague explanation, we consider Eq. (2.4) and rewrite it as

$$(\Omega^{-1} - 1)\rho_{\text{inf}}a^2 = \frac{-3k}{8\pi G}, \quad (2.58)$$

where $\Omega = \Omega_m + \Omega_\Lambda$ during inflation and ρ_{inf} is the energy density of the inflaton field. As ρ_{inf} stays nearly constant during inflation, a^2 grows rapidly and the right hand side of Eq. (2.58) is constant, $\Omega^{-1} - 1$ must decrease over time. Therefore, any initial value of $|\Omega^{-1} - 1|$ can be decreased, when the duration of inflation is long enough, in order to serve as the initial condition for our observed curvature density [14].

At this point, we investigated how inflation can provide us with a spatially flat Universe and a CMB with small temperature fluctuations. The last missing thing is now a seed for structure in our Universe. An imprint of the large scale structure can be seen in the power spectrum of the CMB and, therefore, the shape must have been prepared early on in the Universe. Due to quantum field theory, we know that even in a vacuum quantum fluctuations happen, i.e. the creation and annihilation of particle anti-particle pairs. This process also happens during inflation and because of the rapid expansion of space during that epoch, the quantum fluctuations got swept up and produced perturbations in the early Universe. These perturbations functioned as gravitational instabilities and led to a collapse of some areas, which during the evolution of the Universe formed galaxies and larger structures².

2.3.4 Thermal history of the Universe

Now that we have our standard model of cosmology fixed and extended by an epoch of inflation in the early Universe, we briefly discuss the different stages our Universe passed through during the evolution of the last 13 billion years. For this summary, we go forward in time, i.e. we start at the Big Bang and end today.

²This is only a brief illustration of the process of large scale structure formation. A more detailed description is given in the literature. For the interested reader see [11].

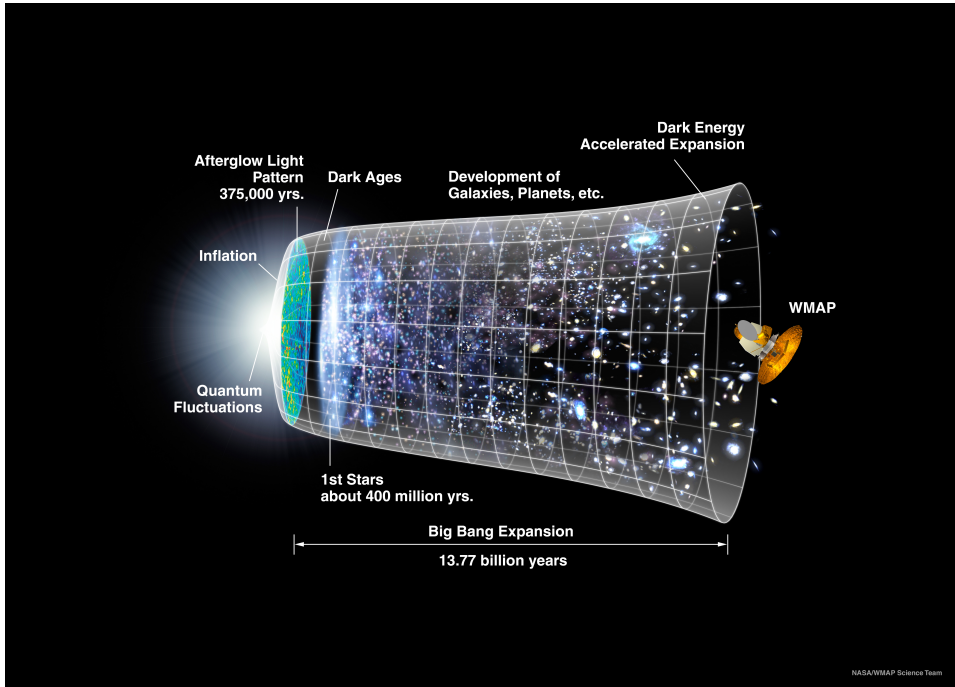


Fig. 2.6. Timeline of the history of our Universe described by the Λ CDM model with an additional epoch of inflation [15].

The Big Bang, Unified Theory and inflation

The beginning of the Universe is supposed to be a Big Bang, an initial singularity. The necessity of having such a Big Bang arises from the current theoretical description of our Universe. Each type of energy present in the Universe has a singularity at cosmic time $t = 0$ in common, where this singularity is the Big Bang and supposed to be the beginning of space and time. After this singularity or to be more precise at least a Planck time $t_{\text{PL}} = 5.39 \cdot 10^{-44}$ s after, our known physical laws set in and it is assumed that we enter an era of one unified force. This unified force is described by a Grand Unified Theory, which combines the strong, electromagnetic and weak force into one. An exact description of this theory has still to be found and a possible description of quantum gravity might enter here as well. The temperature at this epoch is of the order 10^{15} GeV.

After a small time period, the dominant matter in the Universe starts to accelerate the expansion of the Universe rapidly. Supposedly the inflaton field is the only dominant energy component in the Universe during this early stage. It is set in its potential at an arbitrary point and starts to roll down the potential, which accelerates the expansion and the Universe grows rapidly (compare Chapter 2.3.1). During this time, the seeds for structure formation are spread across the Universe. Quantum fluctuations appear in the vacuum of the Universe

and get physically disconnected such that they cannot annihilate each other again and are left over as seeds for gravitational instabilities. The point of losing physical connection is called horizon crossing, because the wavelength of the perturbation becomes larger than the Hubble horizon at that time (compare Fig. 2.7). The scale of these fluctuations is used as a reference in analytical methods of the CMB to constrain inflation and is called pivot scale k_* . As the slow-roll parameter ϵ approaches one, inflation ends. This epoch of inflation lasts from roughly 10^{-35} s to 10^{-33} s after the Big Bang, where the exact time is model dependent.

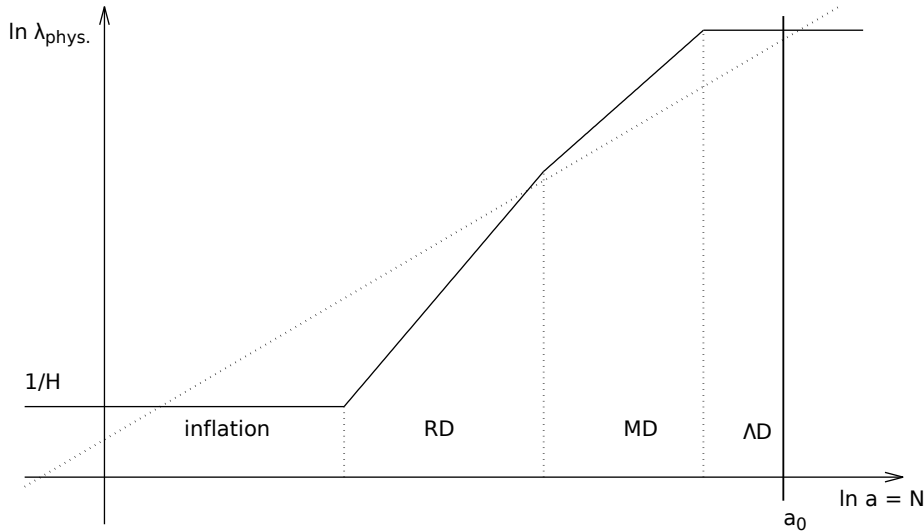


Fig. 2.7. Kinematics of scales. The straight line represents a physical wavelength which grows due to the expansion of the Universe in a linear way. The four different sections show the different epochs of the Universe, inflation, radiation domination (RD), matter domination (MD) and Dark Energy domination (AD). As the physical wavelength becomes larger than the Hubble horizon, the wavelength becomes super horizon and the first horizon crossing occurs. The second time the wavelength and the Hubble horizon are crossing, the physical wavelength becomes sub-horizon again and functions as a seed of gravitational instabilities. The a_0 denotes the present day.

Reheating and radiation domination

As inflation ends, we are left with a Universe that has only the inflaton field in the minimum of its potential and is spatially flat. Now a process sets in which will provide us with particles like those of the standard model of particle physics, filling up the Universe. This process is called pre- or reheating and arises from the fact that the inflaton field misses the minimum,

because of its kinetic energy. One can imagine this as a damped pendulum, which oscillates around its minimum and approaches it with each swing taken. In the case of the inflaton field, this dampening and a coupling to the fields of the standard model of particle physics produces radiation, which starts to fill up the Universe. The exact quantum field theoretical process is still unknown and the description given here is to illustrate a possible way. With this process the inflaton field loses energy and more and more radiation fills up the Universe, which is why we enter the stage of a radiation dominated Universe. Also during this epoch, the strong force should decouple from the other two, where the exact process is unknown. The temperature during and at the end of reheating is unknown, but should be of the order of $10^{15} - 10^9$ GeV. The name reheating arises from the fact that the scalar field can hardly be connected with a temperature and, therefore, the reheating process heats up the Universe after the possible initial heat of the Big Bang decreased due to inflation.

With the reheating process, the Universe is filled with all particles of the standard model of particle physics and at roughly 1 ns, correspondingly 200 GeV, the electroweak force separates into the electromagnetic and the weak force. Around the same time, the Higgs mechanism occurs, which provides the particles with masses, because of the spontaneous symmetry breaking of the Higgs field. This process, which is most likely a crossover, is one of a few phase transitions which occur during the evolution of the Universe. The Universe at that stage is a plasma filled up with photons, neutrinos, quarks, gluons, W- and Z-bosons, electrons, myons and taus, as well as some bound states, which are destroyed quickly, because of the high temperature. The first bound states form as the Universe approaches an age of roughly 1 μ s, which is a temperature of 155 MeV. At this temperature the QCD phase transition occurs. Quarks and gluons form a plasma at high temperature, but at 155 MeV the quarks are confined in colourless bound states, called hadrons. Therefore, some of the ingredients to form nuclei are abundant, but the temperature is still too high to allow such bound states to survive.

Neutrino decoupling and Big Bang Nucleosynthesis

With hadrons being now part of the Universe, and cooling down as expansion goes on, the Universe reaches a temperature at which the interaction rate of the neutrinos becomes smaller than the Hubble expansion. Neutrinos are scattered by their interactions with electrons and positrons,

$$e^- + e^+ \leftrightarrow \nu_e + \bar{\nu}_e. \quad (2.59)$$

The rate of this reaction depends on the number density of electrons and positrons; for relativistic electrons the number density is proportional to the temperature cubed, $n \propto T^3$. Im-

portant for interactions is the cross section of the process, which is for the weak interaction with electrons approximately given by $\langle \sigma v \rangle \sim G_F^2 T^2$, where σ is the cross section, v is the velocity and G_F is the Fermi constant. Combining the cross section and the number density yields the interaction rate Γ , which is

$$\Gamma = n \langle \sigma v \rangle \sim G_F^2 T^5. \quad (2.60)$$

This rate can now be compared to the Hubble rate given by Eq. (2.4), where we neglect terms of curvature and Dark Energy. The energy density during the time of neutrino decoupling is still radiation dominated, so we can use $\rho \propto T^4$. The comparison of the interaction rate and the Hubble rate reads

$$G_F^2 T^5 \sim \sqrt{G T^4}, \quad (2.61)$$

with G the gravitational constant and which is solved for the temperature to

$$T \sim \left(\frac{\sqrt{G}}{G_F^2} \right)^{1/3} \sim 1 \text{ MeV}. \quad (2.62)$$

So at a temperature of roughly 1 MeV the neutrino interaction rate becomes smaller than the expansion rate of the Universe and the neutrinos can start to stream freely. The temperature of 1 MeV corresponds to roughly 1 s after the Big Bang. This process will be discussed again for the photons, from which the CMB is formed. Vice versa, the neutrino decoupling produces a background radiation consisting of neutrinos, like a cosmic neutrino background (CNB or CνB).

As the process of neutrino decoupling is statistical because the temperature and phase can vary locally, the process we will discuss now may occur at the same time. The process of Big Bang Nucleosynthesis describes how the first primordial nuclei were formed from the hadrons in the Universe. Important for this process is the energy scale of binding energies in nuclear physics, which is of the order of 1-10 MeV. At higher temperature the two cases of β -decay are important and leave a ratio of roughly 1:1 between protons and neutrons,



As the temperature decreases due to the expanding Universe, this ratio changes in favour of the protons (because free neutrons are heavier and not stable) and as the Universe approaches temperatures which are smaller than typical binding energies in nuclear physics light atoms such as hydrogen, helium-4, helium-3 and lithium-7 form, where most of those formed atoms

are helium-4. Due to the mean lifetime of neutrons of 880 s, the mass fraction of helium-4 is about 25%, i.e. 8% of all atoms are helium-4 and the rest is mostly hydrogen. The Big Bang Nucleosynthesis happens roughly from 1 s after the Big Bang up to 300 s, which is a temperature range from 1 Mev down to 80 keV. During this process, the photons are still part of the thermal bath and interact with the electrons, positrons and nuclei.

Matter-radiation equality and recombination

As more and more nuclei are formed, which are non-relativistic, the matter density increases and in the same moment the energy density of radiation decreases. At some point during the evolution, both energy densities are the same. This moment is called matter-radiation equality. We can calculate the redshift of matter-radiation equality,

$$1 + z_{\text{eq}} = \frac{\Omega_m}{\Omega_r}, \quad (2.65)$$

where both density parameters are evaluated today and, therefore, we can plug in some values to get the value of the redshift $1 + z_{\text{eq}} = 3365$ [10], which can be converted into a temperature of 0.7 eV and a time of 57000 years after the Big Bang. From the end of inflation up to this point during the evolution of our Universe it was radiation dominated and from this point forward it is dominated by matter.

Since the production of radiation during reheating, photons are in thermal equilibrium with the rest of the Universe. As the temperature of the Universe further decreases, at some point the electrons and atomic nuclei form bound states, as the temperature is not high enough to ionize them again. This formation process of the first atoms is called recombination. Due to this process, the number of free electrons in the Universe drops rapidly and thus the interaction rate for photons becomes small as well. As we already discussed in the context of neutrino decoupling, the photons are separated from the thermal bath and can, therefore, free stream, which we can observe as the CMB today. The temperature of recombination can be found to be roughly 0.26 eV and accordingly can be dated to 370000 years after the Big Bang.

Star formation and accelerated expansion

As we are left with the light atoms, free streaming photons, free streaming neutrinos and some light elements, the Universe becomes dark, because photons are not reflected anywhere. This epoch is known as the Dark Ages and is first disturbed as the quantum fluctuations being super horizon until now, become sub-horizon and form gravitational instabilities at which the nearly homogeneously distributed matter collapse and form stars. The first massive stars have only a

short life time until they explode into supernovae, which form the heavier elements we know and also black holes³. The Dark Ages last roughly until one billion years after the Big Bang.

A last important break point during the evolution of the Universe is the transition into an accelerated expansion. In 1997, Saul Perlmutter, as well as Adam G. Riess, Brian P. Schmidt and others, analysed observations of supernovae of Type Ia⁴, which are used as standard candles in the Universe. The luminosity of supernova type Ia is always the same, due to the fact that a white dwarf explodes. Interesting in their analysis was that close by supernovae (redshifts from 0.16 to 0.62) were moving away faster than expected by Hubble expansion [16, 17]. The three physicists mentioned here were awarded with the Nobel Prize in physics in 2011. Currently, the most prominent explanation of this accelerated expansion is the cosmological constant Λ , which acts as Dark Energy and works against gravity.

³The whole process of star formation and death of a star is a large and interesting topic of astrophysics, but will not be discussed in this thesis.

⁴Supernovae type Ia are unique as the spectrum of them has no hydrogen or helium lines.

Revisiting the number of e-folds of inflation

3

With knowledge of the basics of inflation and the history of the evolution of the Universe as well as observations, we will investigate in more detail how we can test inflation. One big problem is that the potential of inflation is not fixed. So, there are quite a few different models of inflation, which use different terms for the potential, the simplest being $V(\phi) = m^2\phi^2$. We already discussed that the quantum fluctuations during inflation left an imprint on the CMB, which was observed for example by the Planck satellite. The measured power spectrum can be reduced to the initial power spectrum of the fluctuations by assuming a model for these perturbations. The simplest model, therefore, is a power law, i.e.,

$$\mathcal{P}(k) = A_s \left(\frac{k}{k_*} \right)^{n_s - 1}, \quad (3.1)$$

where k is the observed scale, k_* is a reference scale called pivot scale and n_s is the spectral index. Besides the spectral index, we can also measure the running of the spectral index α_s and the ratio between tensor and scalar perturbations r (short tensor-to-scalar ratio). The shape of the power spectrum, meaning the spectral index, is also determined by the number of e-folds at which a given scale becomes super horizon, i.e. this physical mode was larger than the Hubble scale and, therefore, cannot annihilate itself again leading to the already mentioned seeds of gravitational instabilities. According to this, the spectral index and the number of e-folds are connected, e.g. for $m^2\phi^2$ -inflation the relation is $n_s - 1 \approx 1/(2\mathcal{N})$ [18, 19]. In general, $n_s = n_s(\mathcal{N})$ and thus the exact relation depends on the inflationary model. Due to this relation, we can calculate \mathcal{N} for a chosen model of inflation and a pivot scale and compare this with the measurements. This procedure is done by the Planck collaboration and constraints on inflation were given [20]. Also, the number of e-folds \mathcal{N} of a certain pivot scale k_* was used and calculated for different inflationary models,

$$\mathcal{N}(k_*) \approx 67 - \ln\left(\frac{k_*}{a_0 H_0}\right) + \frac{1}{4} \ln\left(\frac{V_*^2}{M_{\text{PL}}^4 \rho_{\text{end}}}\right) + \frac{1 - 3w_{\text{int}}}{12(1 + w_{\text{int}})} \ln\left(\frac{\rho_{\text{th}}}{\rho_{\text{end}}}\right) - \frac{1}{12} \ln(g_{\text{th}}), \quad (3.2)$$

where $a_0 H_0$ is the present Hubble scale, V_* is the potential of k_* at horizon crossing, ρ_{end} is the energy density at the end of inflation, w_{int} parametrizes the effective equation of state during

the reheating process [21] up to a thermalization energy scale ρ_{th} , and g_{th} is the number of effective bosonic degrees of freedom at the energy density ρ_{th} .

In the future, more experiments are planned to make more precise measurements of the CMB such as CMB Stage 4 [22] or LiteBIRD [23]. With these upcoming experiments, we will be able to constrain the error of the spectral index down to $\Delta n_s = \pm 0.0017$ and give a 1σ interval for α_s from -0.018 to $+0.009$ [22]. For $m^2\phi^2$ -inflation this measurement errors lead to an error in the number of e-folds of $\Delta \mathcal{N} = \pm 0.8147$. Providing this precision, we require an accuracy of at least the first decimal in Eq. (3.2). Therefore, we will reconstruct Eq. (3.2), calculate the exact value of 67 and give the required steps to arrive at that equation. As we observe the CMB to constrain inflation, we will also investigate how effects in the evolution of the Universe between first and second horizon crossing might influence the reconstruction.

3.1 Deriving the exact value

To start, we use the definition of a comoving wave number $k = aH$ and of the number of e-folds (2.54), but include the comparison between a wave number today and at horizon crossing, instead of the end of inflation down to horizon crossing [24],

$$\frac{k_*}{a_0 H_0} = e^{-\mathcal{N}(k_*)} \frac{a_{\text{end}}}{a_{\text{eq}}} \frac{H_*}{H_{\text{eq}}} \frac{a_{\text{eq}} H_{\text{eq}}}{a_0 H_0}, \quad (3.3)$$

where the index 'end' denotes end of inflation, the index 'eq' represents the point of matter-radiation equality and the star stands for the point of horizon crossing. For this calculation, we have to include important break points during the evolution of the Universe, which changed that evolution significantly. We already incorporated in Eq. (3.3) the change at the end of inflation and the switch from a radiation dominated epoch into a matter dominated one. Another important break point is the process of reheating. An addition of inflation solves some of the weaknesses of the Λ CDM model, but it introduces another problem, which is the need of a process to form particles from the inflaton field. In the following, we first neglect the reheating process and introduce it later on.

3.1.1 Sudden reheating

Though, the exact process of reheating is rather unknown and still an aspect of research, the influence on the reconstruction of inflation can be large. Therefore, it is important to introduce it later again. However, for the first approach we choose a sudden reheating process, i.e. the particle production from the inflaton field is instantaneous or indistinguishable from a

perfect radiation dominated epoch, so we skip directly from the era of inflation to a radiation dominated one.

For the calculation, we start with Eq. (3.3) and rearrange it,

$$\mathcal{N}(k_*) = -\ln\left(\frac{k_*}{a_0 H_0}\right) + \ln\left(\frac{a_{\text{end}}}{a_{\text{eq}}}\right) + \ln\left(\frac{H_*}{H_{\text{eq}}}\right) + \ln\left(\frac{a_{\text{eq}} H_{\text{eq}}}{a_0 H_0}\right). \quad (3.4)$$

To continue, we need a relation between the scale factor at a radiation dominated epoch and the energy density during the same epoch. For this purpose, we use the assumption that our Universe expanded adiabatically after inflation, so we start off by using that the entropy density s in a comoving volume is constant, i.e. $d(sa^3) = 0$, with

$$s(T) = \frac{2\pi^2}{45} h_{\text{eff}} T^3, \quad (3.5)$$

where h_{eff} are the effective entropy degrees of freedom of all relativistic particles at temperature T . For relativistic particles, we know the energy density ρ as a function of temperature,

$$\rho(T) = \frac{\pi^2}{30} g_{\text{eff}} T^4, \quad (3.6)$$

where g_{eff} are the effective energy degrees of freedom similar to h_{eff} . Now, we replace T in Eq. (3.5) by ρ via Eq. (3.6) and combine $d(sa^3) = 0$ with the result from this replacement and find the relation we wanted,

$$a \propto \rho^{-1/4} g_{\text{eff}}^{1/4} h_{\text{eff}}^{-1/3}. \quad (3.7)$$

Inserting Eq. (3.7) into Eq. (3.4) and separating all known and unknown terms we find

$$\mathcal{N}(k_*) = -\ln\left(\frac{k_*}{a_0 H_0}\right) + \frac{1}{4} \ln\left(\frac{H_*^4 g_{\text{end}}}{\rho_{\text{end}} h_{\text{end}}^{4/3}}\right) + \frac{1}{4} \ln\left(\frac{\rho_{\text{eq}} h_{\text{eq}}^{4/3}}{g_{\text{eq}} H_{\text{eq}}^4}\right) + \ln\left(\frac{a_{\text{eq}} H_{\text{eq}}}{a_0 H_0}\right). \quad (3.8)$$

The last term $(a_{\text{eq}} H_{\text{eq}})/(a_0 H_0)$ can be calculated via the first Friedmann equation (2.35) in the form

$$\frac{H_{\text{eq}}}{H_0} \frac{1}{1+z_{\text{eq}}} = \sqrt{(1+z_{\text{eq}})^2 \Omega_R + (1+z_{\text{eq}}) \Omega_m + \Omega_k + \frac{\Omega_\Lambda}{(1+z_{\text{eq}})^2}} = 218.646 \Omega_m h. \quad (3.9)$$

With Eqs. (2.50), (3.9) and current measurements [10], we can replace the Hubble rate at horizon crossing H_* by the potential V_* and calculate all equality terms in Eq. (3.8) and find

$$\mathcal{N}(k_*) = 66.7228 - \ln\left(\frac{k_*}{a_0 H_0}\right) + \frac{1}{4} \ln\left(\frac{V_*^2 g_{\text{end}}}{M_{\text{PL}}^4 \rho_{\text{end}} h_{\text{end}}^{4/3}}\right). \quad (3.10)$$

This equation connects the number of e-folds of a given model with a chosen pivot scale, we observe today.

3.1.2 Including a reheating process

Now that we have derived the case without a reheating process, we want to include this process in this approach. Therefore, we will assume the more general case, when reheating is not radiation dominated. For this assumption, we can use a parametrization by an averaged equation of state w_{int} [21], because the exact process is unknown.

During the previous calculation, we hid the reheating process in the radiation dominated epoch. To correct this mistake, we have to subtract the perfect radiation dominated case and add the real one,

$$\begin{aligned} \mathcal{N}(k_*) &= -\ln\left(\frac{k_*}{a_0 H_0}\right) + \ln\left(\frac{a_{\text{end,RD}}}{a_{\text{eq}}}\right) + \ln\left(\frac{H_*}{H_{\text{eq}}}\right) + \ln\left(\frac{a_{\text{eq}} H_{\text{eq}}}{a_0 H_0}\right) \\ &\quad + \ln\left(\frac{a_{\text{end,real}}}{a_{\text{reh,real}}}\right) - \ln\left(\frac{a_{\text{end,RD}}}{a_{\text{reh,real}}}\right). \end{aligned} \quad (3.11)$$

As in Chapter 3.1.1, we once again replace the scale factor in the radiation dominated case by the corresponding energy density via Eq. (3.7),

$$\begin{aligned} \mathcal{N}(k_*) &= -\ln\left(\frac{k_*}{a_0 H_0}\right) + \ln\left(\frac{a_{\text{end,RD}}}{a_{\text{eq}}}\right) + \ln\left(\frac{H_*}{H_{\text{eq}}}\right) + \ln\left(\frac{a_{\text{eq}} H_{\text{eq}}}{a_0 H_0}\right) \\ &\quad + \ln\left(\frac{a_{\text{end,real}} \rho_{\text{end}}^{1/4}}{a_{\text{reh,real}} \rho_{\text{reh}}^{1/4}}\right) - \frac{1}{4} \ln\left(\frac{h_{\text{reh}}^{4/3} g_{\text{end}}}{h_{\text{end}}^{4/3} g_{\text{reh}}}\right). \end{aligned} \quad (3.12)$$

The mixed term, containing scale factors as well as energy densities, where the energy densities are in the radiation dominated case and the scale factors give the real case, can be expressed by w_{int} , which is connected to a parameter R_{rad} , an indicator for the deviation from the perfectly radiation dominated reheating process [21],

$$\ln(R_{\text{rad}}) \equiv \ln\left(\frac{a_{\text{end,real}} \rho_{\text{end}}^{1/4}}{a_{\text{reh,real}} \rho_{\text{reh}}^{1/4}}\right) = \frac{1 - 3w_{\text{int}}}{12(1 + w_{\text{int}})} \ln\left(\frac{\rho_{\text{reh}}}{\rho_{\text{end}}}\right). \quad (3.13)$$

For $R_{\text{rad}} = 1$ the reheating process is perfectly radiation dominated and the additional term vanishes. Now, that we have included a reheating process, we apply all steps done in Chapter 3.1.1 to arrive at Eq. (3.10). We get an equation similar to Eq. (3.2), but with an exact value in front and a more precise distinction of the degrees of freedom after reheating,

$$\begin{aligned} \mathcal{N}(k_*) &= 66.7228 - \ln\left(\frac{k_*}{a_0 H_0}\right) + \frac{1}{4} \ln\left(\frac{V_*^2}{M_{\text{PL}}^4 \rho_{\text{end}}}\right) + \frac{1 - 3w_{\text{int}}}{12(1 + w_{\text{int}})} \ln\left(\frac{\rho_{\text{reh}}}{\rho_{\text{end}}}\right) \\ &\quad - \frac{1}{12} \ln\left(\frac{h_{\text{reh}}^4}{g_{\text{reh}}^3}\right). \end{aligned} \quad (3.14)$$

3.2 Change in the reconstruction of number of e-folds due to other effects

As measurement methods become better, we make more precise predictions about primordial fluctuations and the resulting reconstruction of inflation. From this fact, the description of the epoch of inflation improves, but we might come across other effects which possibly influenced the evolution of a pivot scale and are influencing the reconstruction of inflation. In this section, we have a look at how measurement errors affect the reconstruction as well as different additional effects, that changed the evolution of the early Universe.

One assumption we investigate further is slow-roll. In the previous sections, we used single field inflation in a slow-roll regime. Now, we will drop the slow-roll assumption and study how this might affect the reconstruction. A second effect arises from an aspect beyond the standard model of particle physics. For the calculation of the matter-radiation equality terms, the effective degrees of freedom of neutrinos were used with $N_{\text{eff}} = 3.046$, but current research leaves an uncertainty ΔN_{eff} to these degrees of freedom. We analyse the impact of this uncertainty. An important fact of modern cosmology is the accelerated expansion of the Universe in recent times. Current state of research is that the cosmological constant Λ might be the Dark Energy, which leads to an acceleration of expansion. The case when Λ is not Dark Energy is the last effect we investigate and incorporate into the reconstruction of inflation. Although, these effects are the only ones discussed here, there are more effects to consider, which will be mentioned in the outlook (Chapter 5).

3.2.1 Influence of measurement errors

To calculate the 66.7228 of Eq. (3.10), some cosmological parameters from observations, such as T_0 , $\Omega_m h^2$ and N_{eff} were used. These parameters have an influence on all equality terms.

First, we have a look back at the first Friedmann equation for equality (3.9) and incorporate equality via $\Omega_r(1 + z_{\text{eq}}) = \Omega_m$,

$$\frac{H_{\text{eq}}}{H_0} \frac{1}{1 + z_{\text{eq}}} = \sqrt{2(1 + z_{\text{eq}})\Omega_m + \mathcal{O}(10^{-6})}, \quad (3.15)$$

where the $\mathcal{O}(10^{-6})$ arises from the density parameter of curvature Ω_k and the density parameter of Λ divided by $(1+z_{\text{eq}})^2$. We neglect the small additional term of $\mathcal{O}(10^{-6})$ and calculate $1+z_{\text{eq}}$

from $\Omega_r(1 + z_{\text{eq}}) = \Omega_m$,

$$1 + z_{\text{eq}} = \frac{\Omega_m \rho_c}{\frac{\pi^2}{30} \left(2 + \frac{7}{4} \left(\frac{4}{11} \right)^{4/3} N_{\text{eff}} \right) T_0^4} = \frac{3\Omega_m h^2 H_{100}^2 M_{\text{PL}}^2}{\frac{\pi^2}{30} \left(2 + \frac{7}{4} \left(\frac{4}{11} \right)^{4/3} N_{\text{eff}} \right) T_0^4}, \quad (3.16)$$

where the lower part of the fraction is the energy density ρ today and the outer bracket provides the effective degrees of freedom (compare Eq. (3.6)), in which only the photons and neutrinos contribute. In the derivation, the left-hand side of Eq. (3.15) appears logarithmically and we combine that left-hand side with Eq. (3.16), which leads to

$$\ln \left(\frac{a_{\text{eq}} H_{\text{eq}}}{a_0 H_0} \right) = \frac{1}{2} \ln \left(\frac{\Omega_m^2 h^4 M_{\text{PL}}^2 H_{100}^2}{\frac{\pi^2}{90} h^2 T_0^4 \left(1 + \frac{7}{8} \left(\frac{4}{11} \right)^{4/3} N_{\text{eff}} \right)} \right), \quad (3.17)$$

where the index g denotes that these degrees of freedom arise from the energy density. Also important to notice is that the $N_{\text{eff},g}$ are evaluated today if $m_\nu = 0$. Now, we insert the values for $\Omega_m h^2$, T_0 and N_{eff} and in the same step pull out the ratio between the real value and the one we used for the calculation,

$$\begin{aligned} \ln \left(\frac{a_{\text{eq}} H_{\text{eq}}}{a_0 H_0} \right) &= \frac{1}{2} \ln \left(\frac{\left(\frac{\Omega_m h^2}{0.1428} \right)^2 0.1428^2 M_{\text{PL}}^2 H_{100}^2}{\frac{\pi^2}{90} 0.673^2 \left(\frac{h}{0.673} \right)^2 (2.7255 \text{K})^4 \left(\frac{T_0}{2.7255 \text{K}} \right)^4} \right) \\ &\quad + \frac{1}{2} \ln \left(\frac{1}{1 + \frac{7}{8} \left(\frac{4}{11} \right)^{4/3} 3.046 \frac{N_{\text{eff}}}{3.046}} \right), \end{aligned} \quad (3.18)$$

where we separated the term, because the ratios for T_0 and $\Omega_m h^2$ can be placed outside the brackets by using logarithm laws, but the ratio for N_{eff} requires an expansion around $N_{\text{eff}}/3.046 = 1$. Performing this expansion up to linear order and pulling out all the ratios leaves us with the result for the first equality term,

$$\begin{aligned} \ln \left(\frac{a_{\text{eq}} H_{\text{eq}}}{a_0 H_0} \right) &= 3.8364 + \ln \left(\frac{\Omega_m h^2}{0.1428} \right) - 2 \ln \left(\frac{T_0}{2.7255 \text{K}} \right) - \ln \left(\frac{h}{0.673} \right) \\ &\quad - 0.20455 \left(\frac{N_{\text{eff}}}{3.046} - 1 \right), \end{aligned} \quad (3.19)$$

where the first term of 3.8364 is also the value of the logarithm of the right-hand side in Eq. (3.9).

We also analyse the second equality term from Eq. (3.8). For this calculation we use the

first Friedmann equation again and include the energy density at matter-radiation equality,

$$\begin{aligned} \frac{1}{4} \ln \left(\frac{\rho_{eq} h_{eq}^{4/3}}{9H_{eq}^4 g_{eq}} \right) &= \frac{1}{4} \ln \left(\frac{\pi^2}{1080} \frac{h_{eq}^{4/3} T_0^4}{H_{100}^4 \Omega_m^2 h^4 (1+z_{eq})^2} \right) \\ &= \frac{1}{4} \ln \left(\frac{\pi^6}{8748000} \frac{T_0^{12}}{H_{100}^8 \Omega_m^4 h^8 M_{PL}^4} \left(2 + 2 \frac{7}{8} \frac{4}{11} N_{eff} \right)^{4/3} \left(1 + \frac{7}{8} \frac{4^{4/3}}{11^{4/3}} N_{eff} \right)^2 \right), \end{aligned} \quad (3.20)$$

where the first bracket containing a sum is the entropy degrees of freedom at equality h_{eq} and the second bracket the energy degrees of freedom at equality g_{eq} , which arise from the term $(1+z_{eq})^2$. We once again insert values for $\Omega_m h^2$, T_0 and N_{eff} and place outside the brackets the ratio between the real value and the one we used for the calculation

$$\begin{aligned} \frac{1}{4} \ln \left(\frac{\rho_{eq} h_{eq}^{4/3}}{9H_{eq}^4 g_{eq}} \right) &= 62.8865 + 3 \ln \left(\frac{T_0}{2.7255K} \right) - \ln \left(\frac{\Omega_m h^2}{0.1428} \right) + 0.164058 \left(\frac{N_{eff}}{3.046} - 1 \right) \\ &\quad + 0.20455 \left(\frac{N_{eff}}{3.046} - 1 \right), \end{aligned} \quad (3.21)$$

where logarithm laws were used to expand in terms of N_{eff} .

As both terms appear in Eq. (3.8), the total impact of measurement errors is,

$$\begin{aligned} \mathcal{N}(k_*) &= 66.7228 - \ln \left(\frac{k_*}{a_0 H_0} \right) + \frac{1}{4} \ln \left(\frac{V_*^2}{M_{PL}^4 \rho_{end}} \right) + \frac{1 - 3w_{int}}{12(1+w_{int})} \ln \left(\frac{\rho_{reh}}{\rho_{end}} \right) \\ &\quad - \frac{1}{12} \ln \left(\frac{h_{reh}^4}{g_{reh}^3} \right) + \ln \left(\frac{T_0}{2.7255K} \right) - \ln \left(\frac{h}{0.673} \right) + 0.164058 \left(\frac{N_{eff}}{3.046} - 1 \right). \end{aligned} \quad (3.22)$$

It is important to notice, that the value of $\Omega_m h^2$ does not effect the reconstruction of the number of e-folds and only the errors for h , T_0 and N_{eff} appear.

It is also possible to not use N_{eff} as an input for the calculation done above and instead use the redshift of matter-radiation equality z_{eq} . For this purpose, we use the first Friedmann equation at matter-radiation equality and the definition of equality to calculate the first term,

$$\ln \left(\frac{a_{eq} H_{eq}}{a_0 H_0} \right) = \frac{1}{2} \ln(2\Omega_m(1+z_{eq})^2). \quad (3.23)$$

From this equation, we insert the values for h , Ω_m and $(1+z_{eq})$ and pull out again the ratio given the errors,

$$\ln \left(\frac{a_{eq} H_{eq}}{a_0 H_0} \right) = 3.8364 + \frac{1}{2} \ln \left(\frac{\Omega_m h^2}{0.1428} \right) + \frac{1}{2} \ln \left(\frac{1+z_{eq}}{3365} \right) - \ln \left(\frac{h}{0.673} \right). \quad (3.24)$$

Comparing this result with Eq. (3.19), we conclude that the error of T_0 is replaced by an error in $(1+z_{eq})$. Also, the calculation of the second term simplifies, because we do not have to

include the expression for z_{eq} ,

$$\frac{1}{4} \ln \left(\frac{\rho_{\text{eq}} h_{\text{eq}}^{4/3}}{9H_{\text{eq}}^4 g_{\text{eq}}} \right) = \frac{1}{4} \ln \left(\frac{\pi^2}{1080} \frac{h_{\text{eq}}^{4/3} T_0^4}{H_{100}^4 \Omega_m^2 h^4 (1+z_{\text{eq}})^2} \right). \quad (3.25)$$

Inserting the values for $\Omega_m h^2$, N_{eff} , T_0 and $(1+z_{\text{eq}})$ and pulling out the ratio between the real value and the one used yields,

$$\begin{aligned} \frac{1}{4} \ln \left(\frac{\rho_{\text{eq}} h_{\text{eq}}^{4/3}}{9H_{\text{eq}}^4 g_{\text{eq}}} \right) &= 62.8865 + \frac{1}{2} \ln \left(\frac{T_0}{2.7255 \text{K}} \right) + \frac{1}{2} \ln \left(\frac{1+z_{\text{eq}}}{3365} \right) \\ &\quad - \ln \left(\frac{\Omega_m h^2}{0.1428} \right) + 0.164058 \left(\frac{N_{\text{eff}}}{3.046} - 1 \right), \end{aligned} \quad (3.26)$$

where the error in N_{eff} arises again from h_{eq} and is evaluated at matter-radiation equality. As done before, we now combine both terms, which leads to

$$\begin{aligned} \mathcal{N}(k_*) &= 66.7228 - \ln \left(\frac{k_*}{a_0 H_0} \right) + \frac{1}{4} \ln \left(\frac{V_*^2}{M_{\text{PL}}^4 \rho_{\text{end}}} \right) + \frac{1-3w_{\text{int}}}{12(1+w_{\text{int}})} \ln \left(\frac{\rho_{\text{reh}}}{\rho_{\text{end}}} \right) - \frac{1}{12} \ln \left(\frac{h_{\text{reh}}^4}{g_{\text{reh}}^3} \right) \\ &\quad + \ln \left(\frac{T_0}{2.7255 \text{K}} \right) - \ln \left(\frac{h}{0.673} \right) + 0.164058 \left(\frac{N_{\text{eff}}}{3.046} - 1 \right). \end{aligned} \quad (3.27)$$

This result is the same as Eq. (3.22). Consequently, doing the calculation via the redshift of matter-radiation equality does not influence the procedure directly.

3.2.2 Deviation from slow-roll inflation

In Chapter 2.3.1, we discussed the idea and reasoning of slow-roll inflation. Also, we used the first Friedmann equation in the slow-roll case (2.50) to replace the Hubble rate at horizon crossing H_* with the potential at horizon crossing V_* . Now, we study how the reconstruction is changed, if we consider a non slow-roll case for inflation. For this, we use the general form of the Friedmann equation for the inflaton field (2.46) and the second Friedmann equation as well, which for the inflaton field is

$$\frac{\ddot{a}}{a} = \frac{1}{3M_{\text{PL}}^2} (V - \dot{\phi}^2). \quad (3.28)$$

To start off, we first calculate the time derivative of Eq. (2.46),

$$2H\dot{H} = \frac{1}{3M_{\text{PL}}^2} (\dot{\phi}\ddot{\phi} + \dot{\phi}V'). \quad (3.29)$$

We combine this equation with the Klein-Gordon equation (2.43) to get

$$2H\dot{H} = -\frac{H\dot{\phi}^2}{3M_{\text{PL}}^2}. \quad (3.30)$$

By rearranging this equation we find the definition of the slow-roll parameter (2.51), which can also be used in this case, because inflation is going on as $\varepsilon \neq 1$, but the necessity of $\varepsilon \ll 1$ is not satisfied any more,

$$-\frac{\dot{H}}{H^2} = \frac{\frac{1}{2}\dot{\phi}^2}{H^2 M_{\text{PL}}^2} = \varepsilon. \quad (3.31)$$

We insert this definition into the first Friedmann equation again to find

$$\begin{aligned} H^2 &= \frac{1}{3M_{\text{PL}}^2}(H^2 M_{\text{PL}}^2 \varepsilon + V) = \frac{H^2 \varepsilon}{3} + \frac{V}{3M_{\text{PL}}^2} \\ \Leftrightarrow H^2 &= \frac{V}{3M_{\text{PL}}^2} \left(\frac{1}{1 - \frac{1}{3}\varepsilon} \right). \end{aligned} \quad (3.32)$$

We now use this result to replace H_* by V_* , instead of using Eq. (2.50). Let us analyse the affected term in Eq. (3.8),

$$\frac{1}{4} \ln \left(\frac{H_*^4 g_{\text{end}}}{\rho_{\text{end}} h_{\text{end}}^{4/3}} \right) = \frac{1}{4} \ln \left(\frac{V_*^2 \left(\frac{1}{1-\varepsilon/3} \right)^2 g_{\text{end}}}{\rho_{\text{end}} h_{\text{end}}^{4/3}} \right) = \frac{1}{4} \ln \left(\frac{V_*^2 g_{\text{end}}}{\rho_{\text{end}} h_{\text{end}}^{4/3}} \right) + \frac{1}{2} \ln \left(\frac{1}{1 - \frac{1}{3}\varepsilon} \right). \quad (3.33)$$

From this point, we continue with the usual calculation and our end result receives an additional term,

$$\begin{aligned} \mathcal{N}(k_*) &= 66.7228 - \ln \left(\frac{k_*}{a_0 H_0} \right) + \frac{1}{4} \ln \left(\frac{V_*^2}{M_{\text{PL}}^4 \rho_{\text{end}}} \right) + \frac{1 - 3w_{\text{int}}}{12(1 + w_{\text{int}})} \ln \left(\frac{\rho_{\text{reh}}}{\rho_{\text{end}}} \right) - \frac{1}{12} \ln \left(\frac{h_{\text{reh}}^4}{g_{\text{reh}}^3} \right) \\ &\quad + \ln \left(\frac{T_0}{2.7255 \text{K}} \right) - \ln \left(\frac{h}{0.673} \right) + 0.164058 \left(\frac{N_{\text{eff}}}{3.046} - 1 \right) + \frac{1}{2} \ln \left(\frac{1}{1 - \frac{1}{3}\varepsilon_*} \right). \end{aligned} \quad (3.34)$$

3.2.3 Change in the equation of state of Dark Energy

Until now, we always used the cosmological constant Λ as Dark Energy in the Universe. Furthermore, it is discussed if another component X with a negative equation of state, which is necessary to provide an accelerated expansion, is Dark Energy. This deviation from the case of a constant Dark Energy is discussed and we investigate the influence on the reconstruction of inflation. For the case of an evolving Dark Energy, we use the Chevallier-Polarski-Linder (CPL) parametrization in terms of w_0 and w_a , which was first discussed by Michel Chevallier

and David Polarski [25] and later studied more elaborately by Eric V. Linder [26]. If we include the parametrization for evolving Dark Energy, the Friedmann equation changes,

$$\frac{H_{\text{eq}}}{H_0} \frac{1}{1+z_{\text{eq}}} = \sqrt{(1+z_{\text{eq}})^2 \Omega_r + (1+z_{\text{eq}}) \Omega_m + \Omega_k + \Omega_X (1+z_{\text{eq}})^{1+3w_X} \exp\left(\frac{-3w_a z_{\text{eq}}}{1+z_{\text{eq}}}\right)}, \quad (3.35)$$

where w_X is the evolving equation of state of Dark Energy X given by

$$w_X = w_0 + (1-a)w_a = w_0 + \frac{z}{1+z} w_a \stackrel{\text{eq}}{\simeq} w_0 + w_a. \quad (3.36)$$

We include this approximation and expand Eq. (3.35) in the form,

$$\frac{1}{2} \ln(A+B+C) = \frac{1}{2} \ln\left((A+B)\left(1+\frac{C}{A+B}\right)\right) \approx \frac{1}{2} \ln(A+B) + \frac{1}{2} \frac{C}{A+B}, \quad (3.37)$$

where C is the Dark Energy density parameter at equality and $A+B$ is the sum of the other components of the Universe at equality, which are larger than Ω_X . Therefore, the term $C/(A+B)$ is small and we can expand in it, which leads to

$$\frac{H_{\text{eq}}}{H_0} \frac{1}{1+z_{\text{eq}}} = \sqrt{(1+z_{\text{eq}})^2 \Omega_r + (1+z_{\text{eq}}) \Omega_m + \Omega_k} + \frac{1}{4} \frac{\Omega_X}{\Omega_m} (1+z_{\text{eq}})^{3(w_0+w_a)} e^{-3w_a}. \quad (3.38)$$

Implementing this result yields an additional term,

$$\begin{aligned} \mathcal{N}(k_*) &= 66.7228 - \ln\left(\frac{k_*}{a_0 H_0}\right) + \frac{1}{4} \ln\left(\frac{V_*^2}{M_{\text{PL}}^4 \rho_{\text{end}}}\right) + \frac{1-3w_{\text{int}}}{12(1+w_{\text{int}})} \ln\left(\frac{\rho_{\text{reh}}}{\rho_{\text{end}}}\right) - \frac{1}{12} \ln\left(\frac{h_{\text{reh}}^4}{g_{\text{reh}}^3}\right) \\ &\quad + \ln\left(\frac{T_0}{2.7255 \text{K}}\right) - \ln\left(\frac{h}{0.673}\right) + 0.164058 \left(\frac{N_{\text{eff}}}{3.046} - 1\right) + \frac{1}{2} \ln\left(\frac{1}{1-\frac{1}{3}\epsilon_*}\right) \\ &\quad + \frac{1}{4} \frac{\Omega_X}{\Omega_m} (1+z_{\text{eq}})^{3(w_0+w_a)} e^{-3w_a}, \end{aligned} \quad (3.39)$$

which includes all discussed deviations from the current analysis method that the Planck collaboration used (compare Eq. (3.2)).

Slow-roll evolution

4

In Eq. (3.2), which the Planck collaboration used to test inflationary models, the potential at horizon crossing V_* of a pivot scale appears. So, one has to first choose a certain model of inflation to test it. Therefore, some parameters of the primordial power spectrum of quantum fluctuations are reconstructed from measurements of the CMB, like the spectral index of scalar perturbations n_s , the running of the spectral index α_s and the tensor-to-scalar ratio r comparing tensor and scalar perturbations. From these parameters, one produces exclusion plots, where the most prominent one because of the smallest errors is r versus n_s . For r only an upper limit is known whereas n_s has a value with an errorbar (compare Fig. 4.1).

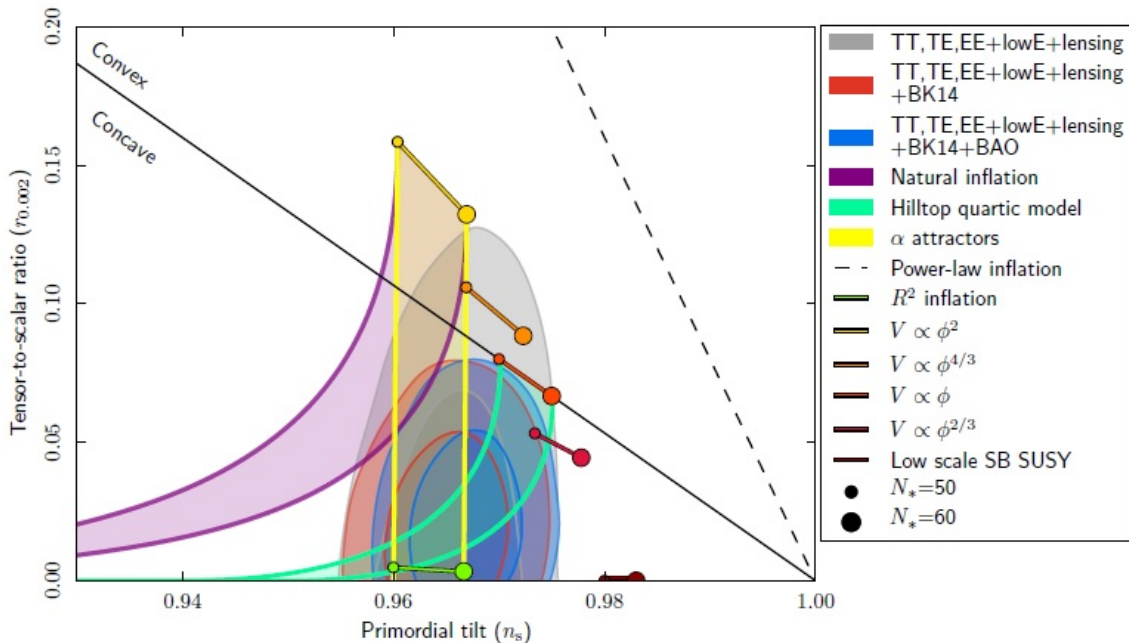


Fig. 4.1. Plot of the tensor-to-scalar ratio versus the spectral index of primordial fluctuations showing how different inflation models fit into the measurements and, therefore, can be accepted or rejected [20]. Shown are both 68% and 95% regions.

In the past, analysis methods used the slow-roll parameters (e.g. (2.51) and (2.52)) to analyse inflation, because Ewan D. Stewart and Jinn-Ouk Gong provided a method to calculate the primordial power spectra for slow-roll models in orders of the slow-roll parameters [27]. With their method, it was possible to calculate the spectra up to second order in terms of slow-roll parameters. As the observational methods became better over time and the method of Stewart and Gong was only applicable to slow-roll inflation, a new set of parameters were introduced by Dominik J. Schwarz, César A. Terrero-Escalante and Alberto A. García. These new parameters describe the Hubble distance and its behaviour during inflation and, therefore, are called horizon-flow parameters $\{\epsilon_n\}$ [28]. The definition is rather simple,

$$\epsilon_{n+1} \equiv \frac{d \ln |\epsilon_n|}{d \mathcal{N}}, \quad n \geq 0, \quad (4.1)$$

where the first parameter ϵ_0 is

$$\epsilon_0 \equiv \frac{d_H(\mathcal{N})}{d_H(\mathcal{N}_i)} = \frac{H_i}{H}, \quad (4.2)$$

where $d_H \equiv 1/H$ denotes the Hubble distance. According to this definition,

$$0 < \epsilon_1 = \frac{d \ln d_H}{d \mathcal{N}}, \quad (4.3)$$

which is the logarithmic growth of the Hubble distance in terms of e-folds and is also the first slow-roll parameter ε given by Eq. (2.51), so inflation happens when $\epsilon_1 < 1$. The definition (4.1) describes a flow in the space $\{\epsilon_n\}$ with the cosmic time as the evolution parameter and the equation of motion

$$\epsilon_0 \dot{\epsilon}_n - \frac{1}{d_{H_i}} \epsilon_n \epsilon_{n+1} = 0. \quad (4.4)$$

As already mentioned, the horizon-flow parameters can be linked to the slow-roll parameters,

$$\begin{aligned} \epsilon_1 &= \varepsilon, \\ \epsilon_2 &= 2\varepsilon - 2\eta, \\ \epsilon_2 \epsilon_3 &= 4\varepsilon^2 - 6\varepsilon\eta + 2\xi^2, \end{aligned} \quad (4.5)$$

where ξ is the third slow-roll parameter. Also, measuring the horizon-flow parameters at a specific moment during inflation provides the value of the potential and its derivatives with respect to the inflaton field. From H and the first three slow-roll parameters the potential and its first two derivatives can be calculated exactly [29],

$$V = 3M_{PL}^2 H^2 \left(1 - \frac{\epsilon_1}{3}\right), \quad (4.6)$$

$$V' = -3M_{PL} H^2 \sqrt{2\epsilon_1} \left(1 - \frac{\epsilon_1}{3} + \frac{\epsilon_2}{6}\right), \quad (4.7)$$

$$V'' = 3H^2 \left(2\epsilon_1 - \frac{\epsilon_2}{2} - \frac{2\epsilon_1^2}{3} + \frac{5\epsilon_1\epsilon_2}{6} - \frac{\epsilon_2^2}{12} - \frac{\epsilon_2\epsilon_3}{6}\right). \quad (4.8)$$

As the power spectra of scalar and tensor perturbations can be expanded in terms of slow-roll parameters by using analytic techniques, it is also possible to expand the power spectra in terms of the horizon-flow parameters. For this, one expands the power spectra around some particular wave number, namely the pivot scale k_* , and then computes the coefficients by using, for example, the slow-roll expansion. The most common expansion variable to cover enough orders of magnitude is $\ln(k_*)$, giving

$$\frac{\mathcal{P}(k)}{\mathcal{P}_0(k_*)} = a_0 + a_1 \ln\left(\frac{k}{k_*}\right) + \frac{a_2}{2} \ln^2\left(\frac{k}{k_*}\right) + \dots \quad (4.9)$$

These coefficients a_n were calculated up to second order in terms of slow-roll parameters for the spectral power spectrum by Stewart and Gong [27] and also up to second order by Liddle, Leach, Martin and Schwarz [29]. For the purpose of this work, we need the spectral indices and the running in the slow-roll approximation, which can be obtained by calculating the logarithm of the power spectra

$$\ln\frac{\mathcal{P}(k)}{\mathcal{P}_0(k_*)} = b_0 + b_1 \ln\left(\frac{k}{k_*}\right) + \frac{b_2}{2} \ln^2\left(\frac{k}{k_*}\right) + \dots \quad (4.10)$$

These first coefficients b_n are linked to the spectral indices and the runnings, because

$$b_{S1} = n_S - 1, \quad b_{T1} = n_T, \quad b_{S2} = \alpha_S, \quad b_{T2} = \alpha_T. \quad (4.11)$$

The expressions in terms of horizon-flow parameters are

$$\begin{aligned} b_{S0} = & -2(C+1)\epsilon_1 - C\epsilon_2 + \left(-2C + \frac{\pi^2}{2} - 7\right)\epsilon_1^2 + \left(-C^2 - 3C + \frac{7\pi^2}{12} - 7\right)\epsilon_1\epsilon_2 \\ & + \left(\frac{\pi^2}{8} - 1\right)\epsilon_2^2 + \left(-\frac{1}{2}C^2 + \frac{\pi^2}{24}\right)\epsilon_2\epsilon_3, \end{aligned} \quad (4.12)$$

$$b_{S1} = -2\epsilon_1 - \epsilon_2 - 2\epsilon_1^2 - (2C+3)\epsilon_1\epsilon_2 - C\epsilon_2\epsilon_3, \quad (4.13)$$

$$b_{S2} = -2\epsilon_1\epsilon_2 - \epsilon_2\epsilon_3, \quad (4.14)$$

with $C = \gamma_E + \ln 2 - 2$, for the scalars and

$$b_{T0} = -2(C+1)\epsilon_1 + \left(-2C + \frac{\pi^2}{2} - 7\right)\epsilon_1^2 + \left(-C^2 - 2C + \frac{\pi^2}{12} - 2\right)\epsilon_1\epsilon_2, \quad (4.15)$$

$$b_{T1} = -2\epsilon_1 - 2\epsilon_1^2 - 2(C+1)\epsilon_1\epsilon_2, \quad (4.16)$$

$$b_{T2} = -2\epsilon_1\epsilon_2, \quad (4.17)$$

for the tensors. We also identify the tensor-to-scalar ratio at the pivot scale

$$\begin{aligned} r = 16\epsilon_1 & \left[1 + C\epsilon_2 + \left(C - \frac{\pi^2}{2} + 5\right)\epsilon_1\epsilon_2 + \left(\frac{1}{2}C^2 - \frac{\pi^2}{8} + 1\right)\epsilon_2^2 \right. \\ & \left. + \left(\frac{1}{2}C^2 - \frac{\pi^2}{24}\right)\epsilon_2\epsilon_3 \right]. \end{aligned} \quad (4.18)$$

With the relation between the spectral indices and the horizon-flow parameters, we use the definition of the horizon-flow parameters (4.1) to get them as a function of the number of e-folds. Therefore, we have to give an initial horizon-flow parameter to start off, because of the recursive definition. As we have to close the set of equations, we use $\epsilon_4 = 0$ and truncate at ϵ_4 . With Eq. (4.1) and $\epsilon_4 = 0$, we calculate $\epsilon_1(\mathcal{N})$ up to $\epsilon_3(\mathcal{N})$,

$$\epsilon_1(\mathcal{N}) = \epsilon_1(0) \exp\left(\frac{\epsilon_2(0)}{\epsilon_3(0)}(\exp(\epsilon_3(0)\mathcal{N}) - 1)\right), \quad (4.19)$$

$$\epsilon_2(\mathcal{N}) = \epsilon_2(0) \exp(\epsilon_3(0)\mathcal{N}), \quad (4.20)$$

$$\epsilon_3(\mathcal{N}) = \epsilon_3(0), \quad (4.21)$$

$$\epsilon_4(\mathcal{N}) = 0. \quad (4.22)$$

In these equations, we have to fix the initial values $\epsilon_1(0)$, $\epsilon_2(0)$ and $\epsilon_3(0)$. We base them on measurements from the Planck satellite for n_S , α_S and r and the Eqs. (4.13), (4.14) and (4.18). We now use Eqs. (4.13), (4.14), (4.18), (4.19), (4.20) and (4.21) to produce parametric plots with the combination of two of those three spectral indices or the tensor-to-scalar ratio. In Fig. 4.2 we show the resulting r versus n_S plot, but without introducing any particular model of inflation. Instead, we show how the different spectral indices and the tensor-to-scalar ratio evolve with changing number of e-folds and changing initial conditions. We use the center value of the Planck measurement $n_S = 0.967$ [10] together with three values for $r < 0.16$ [10], namely $r = 10^{-1}$, $r = 10^{-2}$ and $r = 10^{-3}$. For the values of α_S , we use three different values, namely $\alpha_S = 0$, $\alpha_S = -0.018$ and $\alpha_S = 0.009$, where the last two values correspond to the 1σ sensitivity of CMB Stage 4 [22].

The plot in Fig. 4.2 shows that for values of α_S close to zero, the influence of changing number of e-folds is small, represented by the vertical lines. This small influence makes it difficult to rule out models for the case of small α_S . For a considerable α_S the influence of the number of e-folds becomes larger and for increasing number of e-folds the tensor-to-scalar ratio becomes always smaller, where the increase in the number of e-folds is represented by the arrows. A change in the number of e-folds, increasing for a positive α_S and decreasing for a negative α_S , has a large impact on the spectral index n_S and can help to better constrain inflation. Fig. 4.1 shows that the error in n_S is quite small, which implies for α_S with a considerable value the number of e-folds matter. However, for α_S close to one, a change in the number of e-folds has not a large impact on the spectral indices. With n_S coming close to zero, the influence of the number of e-folds becomes negligible as well.

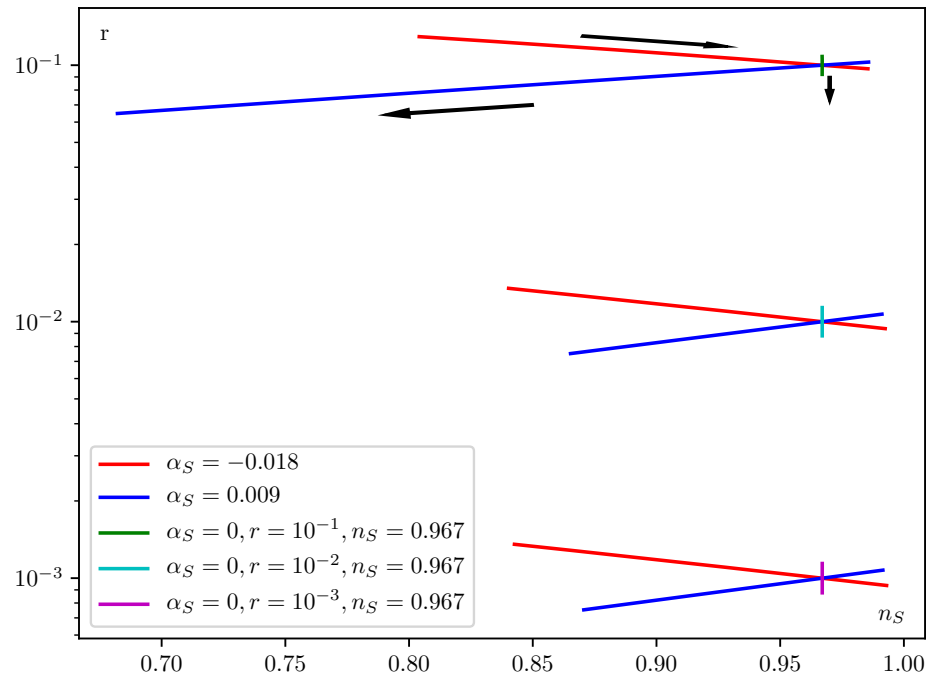


Fig. 4.2. Using the horizon-flow parameters, this graphic shows three different values of r for the same value of n_S , which are the three crossing points. The vertical lines are all using $\alpha_S = 0$, whereas the red lines use $\alpha_S = -0.018$ for the initial value calculation and the blue lines $\alpha_S = 0.009$, which is the 1σ range of CMB Stage 4. The variation in the number of e-folds is ± 4 and the black arrows show the direction of increasing number of e-folds. The arrows are valid for all lines in the plot.

Conclusion and outlook

5

This thesis mainly focused on the aspect of reconstruction of the inflationary epoch in the early Universe. There are two topics I tackled during my time of research, which are first the analysis method used by the Planck collaboration to constrain different inflationary models by utilizing different observables of the CMB and second the approach to avoid the necessity of introducing an inflation model to provide constraints to inflation.

My first point to start off was the Planck publication 'Planck 2018 results. X. Constraints on Inflation' [20], in which Eq. (3.2) was given. As the precision of future observations requires more precision in our analysis methods and from my bachelor thesis I was already working on modifying this equation and including changes due to cosmological effects, such as phase transitions, I wanted to derive the equation first. I was able to derive Eq. (3.2) step by step and by using data from the Planck satellite to give an exact value for the 67, which the Planck collaboration uses (see Eq. (3.14)). A next step was to include the influence of measurement errors, because I used measurements to calculate some equality terms appearing in the derivation. Besides the measurement, I also took other effects into account, which might have occurred during or after inflation and influenced the evolution of our Universe and, therefore, the reconstruction of inflation. One effect is the deviation from slow-roll inflation, which results in a slightly longer duration of inflation. Another effect is additional degrees of freedom, either in the neutrino sector or undiscovered particles, which have a mass small enough to be relativistic at matter-radiation equality. However, the last effect was the discussion about the influence of the cosmological constant Λ not being Dark Energy. All these effects change the reconstruction of inflation and lead to a modified equation,

$$\begin{aligned} \mathcal{N}(k_*) = & 66.7228 - \ln\left(\frac{k_*}{a_0 H_0}\right) + \frac{1}{4} \ln\left(\frac{V_*^2}{M_{\text{PL}}^4 \rho_{\text{end}}}\right) + \frac{1 - 3w_{\text{int}}}{12(1 + w_{\text{int}})} \ln\left(\frac{\rho_{\text{reh}}}{\rho_{\text{end}}}\right) \\ & - \frac{1}{12} \ln\left(\frac{h_{\text{reh}}^4}{g_{\text{reh}}^3}\right) + \ln\left(\frac{T_0}{2.7255 \text{K}}\right) - \ln\left(\frac{h}{0.673}\right) + 0.164058 \left(\frac{N_{\text{eff}}}{3.046} - 1\right) \quad (5.1) \\ & + \frac{1}{2} \ln\left(\frac{1}{1 - \frac{1}{3}\varepsilon_*}\right) + \frac{1}{4} \frac{\Omega_X}{\Omega_m} (1 + z_{\text{eq}})^{3(w_0 + w_a)} e^{-3w_a}, \end{aligned}$$

The discussed effects are only a small selection of possible effects. The biggest effect not mentioned here might be entropy production during the evolution of the Universe, meaning $d(sa^3) = Q$. The adiabatic expansion ($d(sa^3) = 0$) is one of the underlying assumptions of the whole calculation performed in this thesis. Other possible effects are for example, Dark Matter production in the early Universe as well as a super cooling of phase transitions. As all these additional effects might play a roll, we need more observables to test for all these different effects independently. So, besides providing a deeper look into the different effects of the early Universe, this work also leads to the necessity to identify more independent observables to test all those effects.

The second part of this thesis was an approach to avoid the necessity of choosing an inflationary model to give constraints on inflation. This necessity arises from Eq. (5.1), because the potential at horizon crossing appears and forces us to give it a value which depends on the model itself. The method provided in Chapter 4 was developed in collaboration with Truman Emanuel Tapia Mora. The idea is to use the horizon-flow parameters and their link to the spectral indices of the primordial power spectra to avoid the choice of an inflation model. By using the horizon-flow parameters (4.1), we investigate how a change in the number of e-folds changes the set of spectral indices of the spectra. In Fig. 4.2, we only showed the spectral index of scalar perturbations n_s versus the tensor-to-scalar ratio r , which is the common one, because those two parameters are constrained the most. We also only used the running of the spectral index α_s in addition to those two parameters. From the shown method, it is also possible to combine r and α_s or α_s and n_s and change the value of the missing one to see how this impacts the set. As Eq. (4.11) indicates, there are also the spectral index for tensor perturbations n_T and the running of this index α_T , which are not used to calculate the initial conditions for the horizon-flow parameters. These two additional measurements could be used to calculate the horizon-flow parameters as a function of the number of e-folds up to ϵ_5 (by choosing $\epsilon_6 = 0$ as a starting point). Therefore, we need to calculate the coefficients b_n in higher order in terms of ϵ_n , so there are still options to continue this work.

Both of these topics gave me a much deeper understanding of cosmic inflation and how we can get some insight into an epoch which lies behind any observational background and how the observation of the CMB can help by getting this insight and how important those observations of the CMB are.

References

- [1] N. S. H. Hetherington, ed., *Cosmology*, vol. 1634 of *Garland reference library of the humanities ; 1634*, pp. 37–52. New York [u.a.]: Garland, 1993.
- [2] A. H. Guth, “Inflationary universe: A possible solution to the horizon and flatness problems,” *Phys. Rev. D*, vol. 23, pp. 347–356, Jan 1981.
- [3] D. S. Gorbunov, *Hot big bang theory*. 2011.
- [4] S. Weinberg, *Cosmology*, pp. 149–151. Oxford University Press, 2008.
- [5] K. A. Olive *et al.*, “Review of Particle Physics,” *Chin. Phys.*, vol. C38, p. 090001, 2014.
- [6] A. A. Penzias and R. W. Wilson, “A Measurement of Excess Antenna Temperature at 4080 Mc/s.,” *Astrophys. J.*, vol. 142, pp. 419–421, July 1965.
- [7] NASA/WMAP Science Team, “CMB Image.” <https://map.gsfc.nasa.gov/media/121238/index.html>, 2013. [Online; accessed 11-September-2019].
- [8] D. J. Fixsen, “The Temperature of the Cosmic Microwave Background,” *Astrophys. J.*, vol. 707, pp. 916–920, Dec 2009.
- [9] J. Tauber *et al.*, “The Scientific programme of Planck,” 2006.
- [10] N. Aghanim *et al.*, “Planck 2018 results. VI. Cosmological parameters,” 2018.
- [11] A. R. Liddle and D. H. Lyth, *Cosmological inflation and large scale structure*. Cambridge [u.a.]: Cambridge Univ. Press, 2000.
- [12] A. D. Linde, “A new inflationary universe scenario: A possible solution of the horizon, flatness, homogeneity, isotropy and primordial monopole problems,” *Physics Letters B*, vol. 108, pp. 389–393, Feb 1982.

- [13] A. Albrecht and P. J. Steinhardt, “Cosmology for Grand Unified Theories with Radiatively Induced Symmetry Breaking,” *Physics Review Letter*, vol. 48, pp. 1220–1223, Apr 1982.
- [14] P. Coles and G. Ellis, “Is the universe open or closed?,” 1997.
- [15] NASA/WMAP Science Team, “Timeline onf the Universe.” <https://map.gsfc.nasa.gov/media/060915/index.html>, 2012. [Online; accessed 11-September-2019].
- [16] A. G. Riess *et al.*, “Observational evidence from supernovae for an accelerating universe and a cosmological constant,” *Astron. J.*, vol. 116, pp. 1009–1038, 1998.
- [17] S. Perlmutter *et al.*, “Measurements of Ω and Λ from 42 high redshift supernovae,” *Astrophys. J.*, vol. 517, pp. 565–586, 1999.
- [18] V. F. Mukhanov and G. V. Chibisov, “Quantum Fluctuations and a Nonsingular Universe,” *JETP Lett.*, vol. 33, pp. 532–535, 1981. [Pisma Zh. Eksp. Teor. Fiz.33,549(1981)].
- [19] A. A. Starobinsky, “The Perturbation Spectrum Evolving from a Nonsingular Initially De-Sitter Cosmology and the Microwave Background Anisotropy,” *Sov. Astron. Lett.*, vol. 9, p. 302, 1983.
- [20] Y. Akrami *et al.*, “Planck 2018 results. X. Constraints on inflation,” 2018.
- [21] J. Martin and C. Ringeval, “First CMB Constraints on the Inflationary Reheating Temperature,” *Phys. Rev.*, vol. D82, p. 023511, 2010.
- [22] K. N. Abazajian *et al.*, “CMB-S4 Science Book, First Edition,” 2016.
- [23] A. Suzuki *et al.*, “The LiteBIRD Satellite Mission: Sub-Kelvin Instrument,” *Journal of Low Temperature Physics*, vol. 193, pp. 1048–1056, Dec 2018.
- [24] A. R. Liddle and S. M. Leach, “How long before the end of inflation were observable perturbations produced?,” *Phys. Rev.*, vol. D68, p. 103503, 2003.
- [25] M. Chevallier and D. Polarski, “Accelerating universes with scaling dark matter,” *Int. J. Mod. Phys.*, vol. D10, pp. 213–224, 2001.
- [26] E. V. Linder, “Exploring the expansion history of the universe,” *Phys. Rev. Lett.*, vol. 90, p. 091301, 2003.

- [27] J.-O. Gong and E. D. Stewart, “The Density perturbation power spectrum to second order corrections in the slow roll expansion,” *Phys. Lett.*, vol. B510, pp. 1–9, 2001.
- [28] D. J. Schwarz, C. A. Terrero-Escalante, and A. A. Garcia, “Higher order corrections to primordial spectra from cosmological inflation,” *Phys. Lett.*, vol. B517, pp. 243–249, 2001.
- [29] S. M. Leach, A. R. Liddle, J. Martin, and D. J. Schwarz, “Cosmological parameter estimation and the inflationary cosmology,” *Phys. Rev. D*, vol. 66, p. 023515, Jul 2002.

Acknowledgements

At this point, I would like to thank everyone who contributed to this thesis and supported me during the process of researching and writing.

I first like to thank my thesis advisor and first referee Prof. Dominik J. Schwarz, whose office was always open whenever I ran into problems or had a question about my research or writing. He consistently allowed this thesis to be my own work, but steered me in the right direction whenever he thought it was necessary. The possibility to present in the group of cosmology and to hear all the different presentations of my fellow colleagues helped to enlarge my knowledge about different topics of cosmology and astronomy.

I also like to thank Truman Emanuel Tapia Mora, who visited our group and who worked with me on the topic described in Chapter 4. With his help and the discussions we had, it was possible to set up the needed calculations, shown in this thesis, in a week.

Furthermore, I like to thank Dr. Yuko Urakawa, who is the second referee of this thesis, and Prof. Jürgen Schaffner-Bielich from Frankfurt University for crucial input on some topics I got stuck at. Both of them are part of the CRC-211 'Strong-interacting matter under extreme conditions' founded by the Deutsche Forschungsgesellschaft. I am grateful for this CRC, because I am a member of it, which allowed me to stay in Frankfurt for a week and to push my research.

I want to thank Thorben Mense, Miriam Meier, Alexander Klaus, Dr. Aritra Basu and Hendrik Roch for proofreading my thesis and again especially Hendrik Roch for pushing my effort during the writing process.

Eventually, I want to express my special thanks to my family, who supported me throughout my years of study, and to all the other important people who know that they are addressed by reading this.

Declaration of Authorship

I hereby declare that I have written this thesis without the assistance of any other person. The thesis has not been previously submitted to any examination office. Only the sources and literature indicated have been used.

Bielefeld, _____

Pascal Kreling